Michigan Institute for Plasma Science and Engineering (MIPSE)

University of Michigan & Michigan State University

3rd ANNUAL
GRADUATE STUDENT SYMPOSIUM

October 3, 2012

2:00 – 6:00 pm

1345 Engineering Building

Michigan State University

428 S. Shaw Ln., East Lansing, MI 48824

MIPSE 3rd Graduate Student Symposium

October 3, 2012

Schedule

U-M attendees:

12:30 – 12:45	Boarding the bus: SRB, 2455 Hayward Ann Arbor, MI 48109-2143
12:45 – 2:00	Travel to East Lansing
2:00 – 2:15	Posters set up
2:15 – 2:20	***Opening Remarks:*** **Prof. John Verboncoeur** (MSU)
2:20 – 3:05	**Poster Session I**
3:05 – 3:15	**Prof. Satish Udpa**, Dean of Engineering (MSU) ***Overview of COE Research***
3:15 – 4:15	Special MIPSE Seminar: **Prof. Konrad Gelbke** (MSU) ***From NSCL (National Superconducting Cyclotron Facility) to FRIB (Facility for Rare Isotope Beams) at MSU***
4:15 – 5:00	**Poster Session II**
5:00 – 5:45	**Poster Session III**
5: 45 – 6:00	**Best Presentation Award Ceremony**

U-M attendees:

6:00 – 6:15	Boarding the bus: the circle drive off of Red Cedar just North of the Shaw Lane/Red Cedar intersection, East Lansing
6:15 – 7:30	Travel to Ann Arbor

Refreshments will be provided.

mipse

Michigan Institute for Plasma Science and Engineering

Wednesday
October 3, 2012
3:15 pm
Michigan State University
1345 Engineering Building

Prof. Konrad Gelbke

Michigan State University

From NSCL (National Superconducting Cyclotron Facility) to FRIB (Facility for Rare Isotope Beams) at MSU

The NSCL (National Superconducting Cyclotron Facility) is funded by the National Science Foundation under a cooperative agreement to operate NSCL's Coupled Cyclotron Facility (CCF) as a national user facility. NSCL supports research and education in nuclear science, nuclear astrophysics, and accelerator & beam physics and engineering. In 2009, Michigan State University (MSU) and the Department of Energy signed a cooperative agreement to design and establish the Facility for Rare Isotope Beams (FRIB) at MSU, which will advance understanding of rare nuclear isotopes and the evolution of the cosmos. FRIB will be built adjacent to NSCL. CCF operations will cease and the NSCL infrastructure will merge into the FRIB laboratory when FRIB construction nears completion. In this talk, I will provide a high-level summary of the NSCL's current facility and research plans, the envisioned integration into FRIB, the FRIB project status, and emerging new opportunities.

About the Speaker: Konrad Gelbke is a University Distinguished Professor in the Dept. of Physics and Astronomy and Director of NSCL (National Superconducting Cyclotron Laboratory) at Michigan State University. He earned his PhD in physics at the University of Heidelberg in 1973. He spent several years as a researcher at the Max-Planck-Institute for Nuclear Physics in Heidelberg and the Lawrence Berkeley National Laboratory in Berkeley, California before joining NSCL in 1977. Dr. Gelbke has 35 years of experimental nuclear physics experience. His refereed research has been cited 8,700 times and he has an h-index of 54. He has managed over $350 million in funding during his career, 31 years of which have been dedicated to establishing a world-class experimental nuclear physics research program at MSU with collaborators worldwide. As NSCL Director, he focused on advancing rare-isotope science and education at NSCL. Dr. Gelbke has served on the DOE/NSF Nuclear Science Advisory Committee (NSAC), including service as Chair. Dr. Gelbke has served on more than 80 committees worldwide, including writing committees of three consecutive U.S. long range plans for nuclear science, and chairing a major program review for Germany's Helmholtz Association. He is co-initiator of MSU's High Performance Computing Center.

Student Participants

Last Name	First Name	Institution	Poster Session	Poster Number
Asgarian	Mohamad Ali	Michigan State University	III	3-12
Bae	Hyowon	Pusan National University, Korea	I	1-13
Bardel	Charles	Michigan State University	III	3-10
Bell	Iverson	University of Michigan	II	2-10
Demlow	Shannon	Michigan State University	I	1-08
Di Stefano	Carlos	University of Michigan	I	1-06
Frahan	Marc Henry de	University of Michigan	II	2-03
Gucker	Sarah M. Nowak	University of Michigan	I	1-07
Hara	Kentaro	University of Michigan	I	1-02
He	Zhaohan	University of Michigan	II	2-04
Hwang	Seokwon	Pusan National University, Korea	I	1-12
Joglekar	Archis	University of Michigan	III	3-03
Katus	Roxanne	University of Michigan	II	2-13
Kosaka	Hiroyuki	Nagoya University, Japan	II	2-08
Lee	Jung Yeol	Pusan National University, Korea	III	3-01
Liaw	David	University of Michigan	II	2-02
Liu	Peiyao	Michigan State University	II	2-05
Logue	Michael	University of Michigan	I	1-09
Lu	Jing	Michigan State University	III	3-06
MacDonald	Mike	University of Michigan	I	1-04
Meierbachtol	Collin	Michigan State University	I	1-11
Muehle	Matthias	Michigan State University	II	2-09
Parsey	Guy	Michigan State University	III	3-08
Patel	Sonal	University of Michigan	III	3-05
Ranieri	Pietro	University of Michigan	III	3-02
Raymond	Anthony	University of Michigan	III	3-04
Rice	Scott	Michigan State University	II	2-01
Rittersdorf	Ian	University of Michigan	I	1-14
Sommers	Bradley	University of Michigan	II	2-07
Song	In Cheol	Pusan National University, Korea	III	3-11
Song	Sang-Heon	University of Michigan	II	1-03
Tang	Qi	Michigan State University	I	1-01
Tian	Peng	University of Michigan	III	3-09
Tian	Wei	University of Michigan	III	3-07
Vargas	Michael	University of Michigan	I	1-05
Wang	Jun-Chieh (Jerry)	University of Michigan	I	1-10
Winklehner	Daniel	Michigan State University	II	2-12
Wolf	Eric	Michigan State University	II	2-14
Zhang	Peng	University of Michigan	III	3-13
Zhang	Yiting	University of Michigan	II	2-11
Zulick	Calvin	University of Michigan	II	2-06

Poster Session I

1-01	**Qi Tang,** Michigan State University ***High Order WENO AMR Method for Ideal Magnetohydrodynamic Equations***
1-02	**Kentaro Hara**, University of Michigan ***Kinetic Simulations of Partially Magnetized Plasma in a Hall Thruster***
1-03	**Sang-Heon Song,** University of Michigan ***Control of Electron Energy Distributions Through Interaction of Electron Beams and the Bulk in Capacitively Coupled Plasmas***
1-04	**Mike MacDonald**, University of Michigan ***Imaging X-ray Fluorescence Relevant to Hydrodynamic Mixing Experiments at the National Ignition Facility***
1-05	**Michael Vargas**, University of Michigan ***Phase Contrast Imaging with Betatron Radiation from Laser Wakefield Accelerated Electrons***
1-06	**Carlos Di Stefano**, University of Michigan **A Two-Dimensional Multimode RM Experiment on OMEGA-EP**
1-07	**Sarah M. Nowak Gucker**, University of Michigan ***Asymmetric Characteristics of a Dielectric Barrier Discharge***
1-08	**Shannon Demlow**, Michigan State University ***Doping Efficiency in Plasma Enhanced Chemical Vapor Deposition of Boron Doped Diamond***
1-09	**Michael Logue**, University of Michigan ***Control of Ion Energy Distributions Using Ion Mass Ratios in Inductively Coupled Plasmas With a Pulsed DC Substrate Bias***
1-10	**Jun-Chieh (Jerry) Wang**, University of Michigan ***The Role of Micro-Plasmas from Charge Rollers in Printer Engines***
1-11	**Collin Meierbachtol**, Michigan State University ***Including Convective Flows in a Self-Consistent Hydrogen-Based Microwave PACVD Reactor Model***
1-12	**Seokwon Hwang**, Pusan National University, Korea ***Performance Improvement of a Particle-in-Cell Simulation Using GPUs***
1-13	**Hyowon Bae**, Pusan National University, Korea ***Characteristics of Radio-Frequency Driven Discharges in Sub-micro Gap***
1-14	**Ian Rittersdorf**, University of Michigan ***Effects of Random Circuit Fabrication Errors on Small Signal Gain and Output Phase in a Traveling Wave Tube***

Poster Session II

2-01	**Scott Rice,** Michigan State University ***Multipactor Suppression in Resonant Cavities via Secondary Modes***
2-02	**David Liaw,** University of Michigan ***Simulation of Using Background Plasma to Neutralize Charged Particle Thrusters on Nanospacecraft***
2-03	**Marc Henry de Frahan,** University of Michigan ***Beryllium Strength under Extreme Dynamic Loading Conditions***
2-04	**Zhaohan He,** University of Michigan ***Diffraction of Electron Pulses Generated from Laser-Plasma Wakefield***
2-05	**Peiyao Liu,** Michigan State University ***Atmospheric Pressure Microwave-Powered Microplasma Source***
2-06	**Calvin Zulick,** University of Michigan ***Neutron Generation Using Ultra-Intense Laser Plasma Interactions***
2-07	**Bradley Sommers,** University of Michigan ***Plasma Formation Inside Deformed Gas Bubbles Submerged in Water***
2-08	**Hiroyuki Kosaka,** Nagoya University, Japan ***Atomic Composition of Diamond-Like Carbon Film Coated at over 100 □m/h by Using Microwave-Excited High-Density Near Plasma***
2-09	**Matthias Muehle,** Michigan State University ***Quality and Internal Stress of Single Crystalline Diamond Synthesized by Microwave Plasma Assisted Chemical Vapor Deposition***
2-10	**Iverson Bell**, University of Michigan ***Investigating Low Earth Orbit Plasma Interaction to Enhance Understanding of Miniaturized Electrodynamic Tether Propulsion for Femtosatellites and Picosatellites***
2-11	**Yiting Zhang,** University of Michigan ***Ion Energy Angular Phase Distribution from the Bulk Plasma through Sheath in Single- and Dual-Frequency Capacitively Coupled Plasma***
2-12	**Daniel Winklehner,** Michigan State University ***Space Charge Compensation Measurements of Multi-Charged Ion Beams Extracted from an ECR Ion Source***
2-13	**Roxanne Katus,** University of Michigan ***Similarities and Differences in Low-to-Mid Latitude Geomagnetic Indices During Storms***
2-14	**Eric Wolf**, Michigan State University ***Lacunae-Based Stabilization of FDTD Mesh Refinement***

Poster Session III

3-01	**Jung Yoel Lee,** Pusan National University, Korea ***Investigation of EEPFs in a Micro Dielectric Barrier Discharge at Atmospheric Pressure Using a Particle-in-Cell Simulation***
3-02	**Pietro Ranieri,** University of Michigan ***Stimulated Beam Extraction Performance Characterization of a 50-cm Ion Thruster Discharge***
3-03	**Archis Joglekar,** University of Michigan ***Magnetic Reconnection in Plasma under Inertial Confinement Fusion Conditions Driven by Heat Flux Effects in Ohm's Law***
3-04	**Anthony Raymond,** University of Michigan ***Directional, Energetic Neutron Generation via High-Intensity Laser/Plasma Interactions at CUOS***
3-05	**Sonal Patel,** University of Michigan ***X-Pinch Experiments on UM Linear Transformer Drivers***
3-06	**Jing Lu,** Michigan State University ***A Description of the Experimental Microwave Discharge Behavior versus Pressure, Power and Reactor Geometry for MPACVD Diamond Synthesis Reactors***
3-07	**Wei Tian,** University of Michigan ***Simulations of Plasma Dynamics of Electrical Discharges Sustained in Bubbles in Water***
3-08	**Guy Parsey,** Michigan State University ***Kinetic Modeling of Electronically Enhanced Reaction Pathways in Plasma Assisted Combustion***
3-09	**Peng Tian,** University of Michigan ***Controlling Ion and UV/VUV Photon Fluxes in Pulsed Low Pressure Inductively Coupled Plasmas for Materials Processing***
3-10	**Charles Bardel**, Michigan State University ***Increasing Efficiency of Monte Carlo Particle-Fluid Collision Calculations on GPU***
3-11	**In Cheol Song**, Pusan National University, Korea ***Parallelized Two-dimensional Particle-in-cell Simulation for Capacitively cou-pled Plasma Using Graphic Processing Unit***
3-12	**Mohamad Ali Asgarian,** Michigan State University ***Modeling of the O-X-B Double Conversion Pprocess in Fusion Plasmas***
3-13	**Peng Zhang,** University of Michigan ***Spreading Resistance of Thin Film Contacts***

ABSTRACTS
Poster Session I

1-01

High Order WENO AMR Method for Ideal Magnetohydrodynamic Equations

Qi Tang [a], Andrew Christlieb [a], Yaman Guclu [a] and James Rossmanith [b]

(a) Department of Mathematics, Michigan State University (tangqi@msu.edu)
(b) Department of Mathematics, Iowa State University

The ideal magnetohydrodynamic (MHD) equations are the single-fluid model of plasma, important in modeling many phenomena. The fundamental numerical challenges of MHD equations are to preserve conservation and positivity of the density and pressure, satisfy the divergence-free constraint and achieve non-oscillatory solutions when complicated waves appear.

The new WENO AMR algorithm [2] will be used to simulate the ideal MHD Equations and tackle those challenges. The magnetic potential advection constrained transport method (MPACT) [1] will be used to satisfy the divergence-free constraint of magnetic field. The new feature of our WENO AMR algorithm will be (1) the method is finite difference type and able to obtain high-order and high-resolution solutions, (2) all the quantities are treated as ceil-centered such that it is suitable for the AMR framework, (3) all the quantities including the magnetic field will be essentially non-oscillatory, with TVD integrator and WENO reconstruction used. Convergence study will be done on the smooth problem to show high order property of the solver. 1D/2D challenging benchmark problems such as Brio-Wu shock tube problem will be presented in the AMR framework. We expect our algorithm is robust, essentially non-oscillatory and suitable for resolving solution structures, because of the very small numerical diffusion introduced.

References

[1] J. Rossmanith, SISC. **28** 1766 (2006)
[2] C. Shen, J.M. Qiu and A. Christlieb, J. Comp. Phys. **230** 3780 (2011)

1-02

Kinetic Simulations of Partially Magnetized Plasma in a Hall Thruster

Kentaro Hara [a], Iain D. Boyd [a] and Vladimir I. Kolobov [b]

(a) Department of Aerospace Engineering, the University of Michigan (kenhara@umich.edu)
(b) CFD Research Corporation

Due to complex mechanisms such as plasma-wall interaction, collisions, and anomalous diffusion, the partially magnetized plasma in Hall thrusters is known to be in a highly non-equilibrium state. For better understanding of the essential properties of plasma in Hall thrusters, recent numerical simulations and experiments have focused on obtaining the velocity distribution functions (VDFs) or energy distribution functions (EDFs) of plasma species.

In the low temperature plasma community, two computational methods have been developed and used to predict the plasma behavior. Fluid methods use macroscopic quantities, such as density, mean velocity, and temperature, enabling fast computation yet neglecting some important non-equilibrium effects. On the other hand, kinetic solvers, such as the particle-in-cell (PIC) or discrete velocity methods, are able to simulate the non-equilibrium nature of the plasma. However, statistical noise due to the use of macro-particles is mostly unavoidable in particle simulations. In particular, low density regions such as near the electrodes and the tail of VDFs (i.e. the high energy electrons) suffer from inaccurate simulation due to inherent statistical noise.

The key feature of this study is to develop a deterministic kinetic (DK) method that solves the kinetic Boltzmann equation directly by discretizing the phase space, including both physical and velocity spaces. Here, we compare the DK and PIC methods for ions and neutral atoms to simulate the discharge plasma of a SPT-100 Hall thruster. In order to compare the features of the two methods, both kinetic models are used for heavy species and an identical fluid model is used for electrons. The results obtained from the hybrid-DK method is in good agreement with the hybrid-PIC results and experiments in terms of the time averaged plasma properties.[1] However, the differences are seen in the time resolved results. Figure 1 shows the instantaneous VDFs of ions at the channel exit. The DK simulation provides an improved resolution of VDFs and thus temporally/spatially well resolved plasma properties in comparison to the PIC results. In order to reduce the computational cost, GPU computing is considered to be suitable for DK solvers.[2] Currently, we are working on GPU acceleration and applying the DK simulation to other cases.

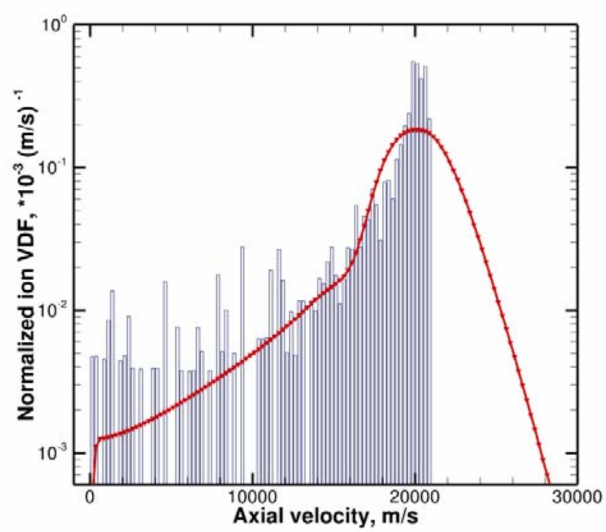

Fig. 1: Instantaneous velocity distribution functions of ions at the channel exit of a SPT-100 Hall thruster (Red solid line: hybrid-DK, Blue histogram: hybrid-PIC)

References

[1] K. Hara, I. D. Boyd, and V. I. Kolobov, AIAA Paper 2012-4313, (2012).

[2] V. I. Kolobov and R. R. Arslanbekov, J. Comput. Phys. **231**, (2012)

1-03

Control of Electron Energy Distributions through Interaction of Electron Beams and the Bulk in Capacitively Coupled Plasmas

Sang-Heon Song [a] and Mark J. Kushner [b]

(a) Nuclear Engineering and Radiological Sciences (ssongs@umich.edu)
(b) Electrical Engineering and Computer Science (mjkush@umich.edu)
University of Michigan, Ann Arbor, MI 48109 USA

The control of electron energy distributions, *f(ε)*, in capacitively coupled plasmas is necessary to optimize the fluxes of reactive species to the substrate in material processing. Under select conditions, beams of electrons with energies >100s eV can be produced by secondary electron emission (by ions, photons, excited states and electrons) and subsequent acceleration through the sheaths. Although the beam electrons are most collisional with the background, collisions of beam electrons with bulk electrons do occur. Previous work has investigated the possibility of beam-Langmuir wave interactions in such systems that may transfer energy to the bulk electrons.[1] In this paper, we report on a computational investigation of the purely kinetic interaction between the beam and bulk through Coulomb electron-electron (e-e) collisions, and the consequences on the *f(ε)*. A single frequency CCP with and without a dc augmentation is investigated with a 2-dimensional plasma hydrodynamics model which includes an Electron Monte Carlo Simulation which resolves e-e collisions. High energy secondary electrons are produced by ion-induced secondary electron emission (i-SEE) and electron-induced SEE (e-SEE). The beam-like secondary electrons collide with low energy electrons in the bulk plasma, delivering energy to the bulk electrons and depleting the beam electrons. This interaction between beam electron and bulk electron can modulate the *f(ε)*, to produce shapes that are not otherwise attainable in self-sustained rf equilibrium plasmas. For example, an *f(ε)* may be produced that has a raised high energy tail component due to the energy transferred from the high energy electrons beam to the low energy bulk electrons. We will discuss shaping of *f(ε)* and changes in plasma properties through the beam-bulk interactions, and how the choice of dc bias on the upper electrode may be a parameter to control the *f(ε)*.

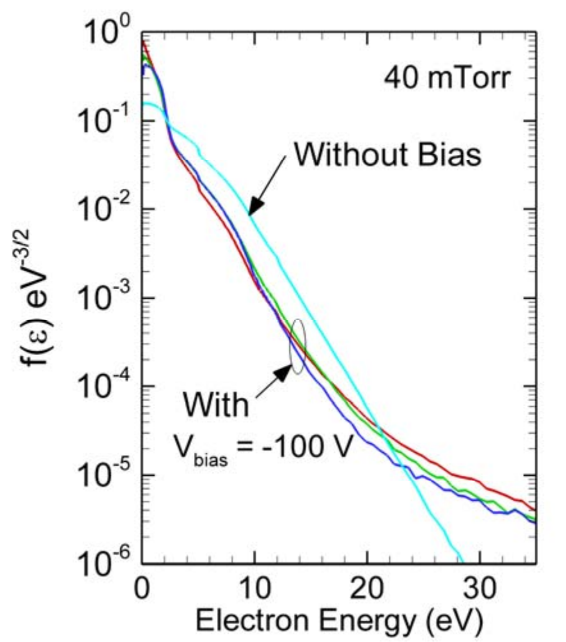

Fig. 1: The electron energy distribution with and without dc bias. The different colors with bias represent various secondary emission coefficients of the biased electrode.

Reference

[1] L. Xu, L. Chen, M. Funk, A. Ranjan, M. Hummel, R. Bravenec, R. Sundararajan, D. J. Economou, and V. M. Donnelly, Appl. Phys. Lett. **93**, 261052 (2008).

1-04

Imaging X-ray Fluorescence Relevant to Hydrodynamic Mixing Experiments at the National Ignition Facility

M.J. MacDonald, E.J. Gamboa, C.C. Kuranz, P.A. Keiter and R.P. Drake

Atmospheric, Oceanic, and Space Science, University of Michigan (macdonm@umich.edu)

The National Ignition Facility (NIF) is capable of providing enough energy to explore areas of physics that are not possible on any previous laser system. This includes large-volume, geometrically complex hydrodynamic and radiation hydrodynamic experiments in which traditional, line-integrated radiographic techniques limit the quality of the results. As an example, we are involved in divergent hydrodynamic experiments at the NIF, motivated by supernova hydrodynamics, that cannot be diagnosed in detail with transmission radiography. X-ray scattering has been considered for this purpose and appears feasible [1]. Here we consider fluorescence imaging, a better candidate as the cross section of photoabsorption in the several-keV range is roughly 100 times larger than that of scattering. A single layer of the target will be uniformly doped with a fluorescent tracer, which will be pumped by a sheet of x-rays. The fluorescent intensity will be measured to create a density map of the doped material as it mixes with other layers. Developing this diagnostic will create a powerful tool to characterize hydrodynamic experiments with complex geometries.

Reference

[1] Huntington et al. High Energy Density Physics 6, 194 (2010).

1-05

Phase Contrast Imaging with Betatron Radiation from Laser Wakefield Accelerated Electrons

Michael Vargas, William Schumaker, Zhaohan He, Vladimir Chvykov, Victor Yanovsky, Anatoly Maksimchuk, Karl Krushelnick, and Alec Thomas

Center for Ultrafast Optical Science, University of Michigan, Ann Arbor, Michigan, 48109

Laser wakefield acceleration is a method of accelerating electrons using a high intensity laser [1]. The laser pulse first ionizes the gas to produce a plasma, where the electrons and ions are dissociated. The electrons are then immediately expelled in the vicinity of the laser pulse due to the ponderomotive force. Ions, being much heavier than the electrons, are too slow to move on the time scale of the laser. This results in a moving positive space charge following the laser. The electric field from this space charge can accelerate electrons behind it to ultra-relativistic energies [2-6]. Additionally, due to transverse electric fields in the wake structure, the accelerated electrons can oscillate in the transverse direction. This acts like a miniature wiggler, producing a beam of synchrotron like x-rays called betatron radiation.

To study this betatron radiation, the HERCULES laser (800nm, 30 fs Ti:Sapphire) at the University of Michigan was used with 160 TW peak power. The beam was focused using either f/10 or f/20 4" off-axis parabolic mirrors onto the front edge of a supersonic conical gas jet (5mm length). The spatially coherent betatron radiation produced by the transverse motion of the accelerated electrons was used for phase contrast imaging of custom fabricated samples. The fabricated samples were built to contain edges (for producing phase contrast), while keeping the material thickness constant in order to eliminate signal variation from x-ray absorption. Two detectors were implemented to produce images at different x-ray energies. Direct detection on an x-ray CCD was used in the lower energy regime (1keV-15keV), while a fiber-coupled scintillator was used to image the higher energy x-rays (3keV- 60keV).

Additionally, phase contrast imaging in both self-injection and ionization-induced injection cases was compared. Ionization induced injection relies on doping the acceleration gas (Helium) with a higher Z dopant (Nitrogen) to increase the trapped charge [7-8]. The dopant gas provides additional seed electrons in the high intensity region of the laser pulse, which are at an ideal location to be injected into the wakefield following the laser pulse. The increase in charge and variation in beam dynamics, when compared with self-injection, affects the betatron radiation emitted by the interaction.

References

[1] T. Tajima and J.M. Dawson, Phys. Rev. Lett. **43**, 267 (1979).
[2] S.P.D. Mangles et al., Phys. Rev. Lett. **94**, 245001 (2005)
[3] V. Malka et al., Science **298**, 1596 (2002)
[4] S.P.D. Mangles, et al., Nature (London) **421**, 535 (2004)
[5] C.G.R. Geddes et al., Nature (London) **421**, 538 (2004)
[6] J. Faure et al., Nature (London) **421**, 541 (2004)
[7] C. McGuffey, A.G.R. Thomas, et al., Phys. Rev. Lett. **104**, 025004 (2010)
[8] A. Pak., K.A. Marsh, et al. Phys. Rev. Lett., **104**, 025003 (2010)

1-06

A Two-Dimensional Multimode RM Experiment on OMEGA-EP

C. A. Di Stefano [a], G. Malamud [a,b], C. C. Kuranz [a], S. R. Klein [a], M. J. Grosskopf [a], P. A. Keiter[a], R. P. Drake[a]

(a) Department of Atmospheric, Oceanic, and Space Sciences, University of Michigan (carlosds@umich.edu)
(b) Department of Physics, Nuclear Research Center – Negev, Beer-Sheva, Israel

The Richtmyer-Meshkov (RM) process occurs when a shock wave crosses an interface between two materials of different densities and deposits vorticity on it due to interface and/or shock-front structure, causing this initial structure to grow in time. This process also occurs when astrophysical shock waves cross density gradients. It has been suggested that RM is responsible for observed structure in the Tycho supernova remnant. Previous HED RM experiments using machined interfaces have examined only single-mode behavior, often in the regime of high Mach number and large amplitude, such that interaction between the RM spikes and the shock is significant. In the case of a multimode initial perturbation, the non-linear bubble-competition process is dominant. This causes the average wavelength of the perturbation to increase with time, and the width of the overall mixing zone to grow faster than in the case of a single-mode interface. At late time, the mixing-zone growth is theorized to become self-similar. Although there have been studies of RM using uncharacterized three-dimensional multimode perturbations, none of this previous work has examined the evolution of a well-characterized multimode interface and its spectral structure in the bubble-merger regime. In the present study, we discuss an experimental design, to be implemented on Omega EP, meant to measure two-dimensional multimode RM evolution at late times with well-characterized initial conditions.

This work is funded by the NNSA-DS and SC-OFES Joint Program in HEDLP, by the NLUF in NNSA-DS and by the PSAAP in NNSA-ASC. The corresponding grant numbers are DE- FG52-09NA29548, DE-FG52-09NA29034, and DE-FC52-08NA28616.

1-07

Asymmetric Characteristics of a Dielectric Barrier Discharge

Sarah M. N. Gucker [a], María C. García [b] and John E. Foster [a]

(a) Department of Nuclear Engineering and Radiological Sciences, University of Michigan (sngucker@umich.edu, jefoster@umich.edu)

(b) Department of Applied Physics, University of Cordoba, Spain (fa1gamam@uco.es)

Low temperature plasmas have become a popular subject of research due to their numerous applications in a variety of fields and technologies. A subset, atmospheric pressure plasmas in liquid water have drawn interest due to their ability to destroy bacterial, viral and inorganic contaminants, sterilizing the liquid.

Discussed here are the results from a study of a dielectric barrier discharge plasma operating in low radio frequencies for a variety of gases. These plasmas exhibit a physical asymmetry over the discharge cycle, which is believed to have a strong effect on the chemical mechanisms. In other words, the physics and chemistry of these plasmas is a highly time-dependent system. To adequately use these plasmas to sterilize and purify water requires an adequate understand of the physics and chemistry of the discharge, thus a dynamic analysis is required. Presented here are various diagnostics, including time-resolved optical emission spectroscopy and fast imaging, key to understanding the plasma's evolution throughout the discharge cycle.

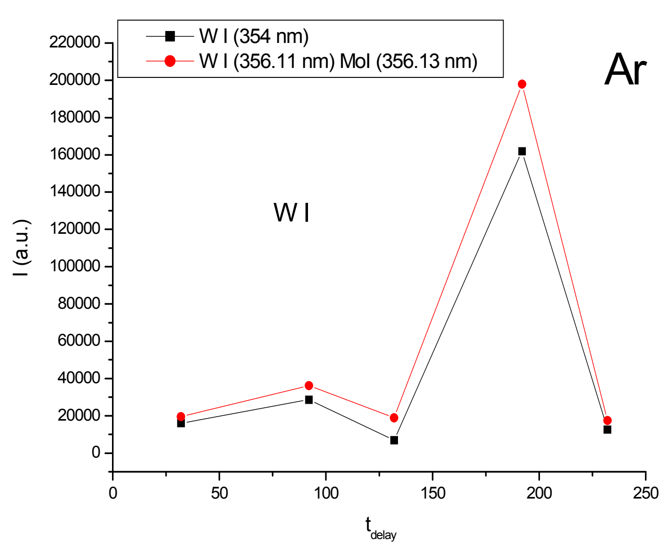

Fig. 1: Asymmetric optical emission. Here, the line intensity for an argon discharge is seen to be asymmetric over a discharge cycle (here, tungsten, the electrode material).

This material is based upon work supported by the National Science Foundation (CBET 1033141) and the National Science Foundation Graduate Student Research Fellowship under Grant No. DGE 0718128.

References

[1] Andreozzi, R., Catalysis Today, **53** (1999).

[2] Gigosos, M. et al., Spectrochim Acta B, **58** (2003).

[3] Foster, J., Sommers, B.S., Gucker, S.N., et al., IEEE T Plasma Sci, **40** (2012).

1-08

Doping Efficiency in Plasma Enhanced Chemical Vapor Deposition of Boron Doped Diamond

Shannon Nicley Demlow [a], Michael Becker [b] and Timothy Grotjohn [a,b]

(a) Michigan State University, Department of Electrical and Computer Engineering, East Lansing, MI, USA

(b) Fraunhofer USA Center for Coatings and Laser Applications, East Lansing, MI, USA

(nicleysh@msu.edu)

With many superior physical and electronic properties, diamond is an ideal candidate for many materials applications. Diamond has enormous untapped potential in electronics, where its high breakdown voltage and wide bandgap would make it particularly well suited to high-temperature and high-power devices, such as boron doped *p*-type diamond Schottky-barrier diodes. Free-standing, heavily-doped (boron concentrations of > 10^{20} cm^{-3}) *p*-type substrates are a precondition for the higher-power vertical diode architectures, and reliably producing these highly-doped substrates will require high growth rates to reduce growth time, and high doping efficiency from boron in the plasma feedgas to the boron incorporated in the grown crystal.

Recent investigations [1] have shown that decreasing doping efficiency at higher pressures (higher plasma discharge power densities) is an obstacle in achieving thick, highly boron-doped films. Achard et al. [1] have theorized that this decrease in doping efficiency is due to the increasing microwave power densities required to achieve a satisfactory growth rate of heavily doped films.

To determine the conditions required to increase the doping efficiency, thin homoepitaxial boron doped diamond films grown in a wide range of plasma chemistries were analyzed. Growth variables such as diborane level in the plasma feedgas were investigated to show their effect on total incorporated boron. The results of this work will be used to inform ongoing research [2] on increasing doping efficiency and growth rates of *p*-type single crystal diamond during plasma-enhanced chemical vapor deposition. The samples grown in this work showed a higher doping efficiency than other recent studies have reported. This may be due to the FTIR method used to determine the boron concentration, as it is sensitive to surface defects, as well as experimental conditions such as a higher surface temperature during growth and a slower growth rate. Future investigations based on the results of this work may allow gains in both doping efficiency and growth rate of *p*-type substrates simultaneously, which may ultimately lead to the realization of high-power, high-temperature diodes.

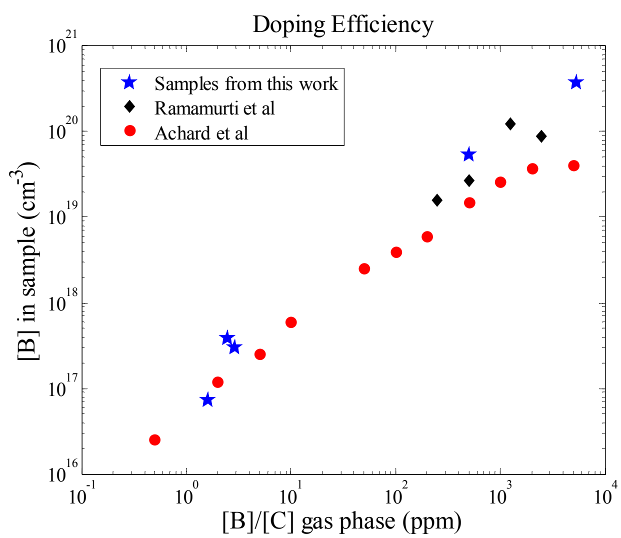

Fig. 1: Doping efficiency is shown graphically for the samples of this work, along with previous results from this group [3] and results from the recent literature [1].

References

[1] J. Achard, *et. al*, *Diam. & Rel. Mater* **20** (2011) 145.

[2] S.N. Demlow, *et. al* MRS Proceedings **1395** (2012) *doi:10.1557/opl.2012.461.*

[3] R. Ramamurti, *et. al*, *Diam. & Rel. Mater.* **17**, (2008) 1320.

1-09

Control of Ion Energy Distributions Using Ion Mass Ratios in Inductively Coupled Plasmas with a Pulsed DC Substrate Bias

Michael D. Logue and Mark J. Kushner

Department of Electrical and Computer Engineering, University of Michigan, Ann Arbor, MI 48109 USA
(mdlogue@umich.edu, mjkush@umich.edu)

In many applications requiring energetic ion bombardment, such as plasma etching, gas mixtures containing several ionic species are used. In cases where two ions have significantly different masses, it could be feasible to selectively control the ion energy distributions (IEDs) of the ions by, for example, preferentially extracting the lighter ion mass with a controllable energy. In this work, we investigate the possibility of using pulsed DC biases of varying formats on the substrate to obtain this control. The applied pulsed bias will shift the plasma potential and modify the IEDs to surfaces without significant changes in the bulk plasma properties. If short enough pulses are used it may be possible to obtain significant flux of the lower mass ionic species at high energy, with negligible flux of the higher mass species at the applied bias potential. A computational investigation of IEDs in low pressure (a few to 100 mTorr) ICPs sustained in Ar/H_2 and Xe/H_2 mixtures (having large mass differences) is being conducted for proof of principle. The investigation is being conducted using the Hybrid Plasma Equipment Model (HPEM) with which electron energy distributions and the IED as a function of position and time are obtained using Monte Carlo simulations. The sustaining ICP power will be applied in continuous and pulsed formats, while the substrate dc voltage will be applied in pulsed format. We have found a selective ability to mass and energy discriminate ion fluxes with sufficiently short bias pulses, as shown in Fig. 1. Results from the model for plasmas densities, electron temperatures, electron distributions and IEDs will be discussed.

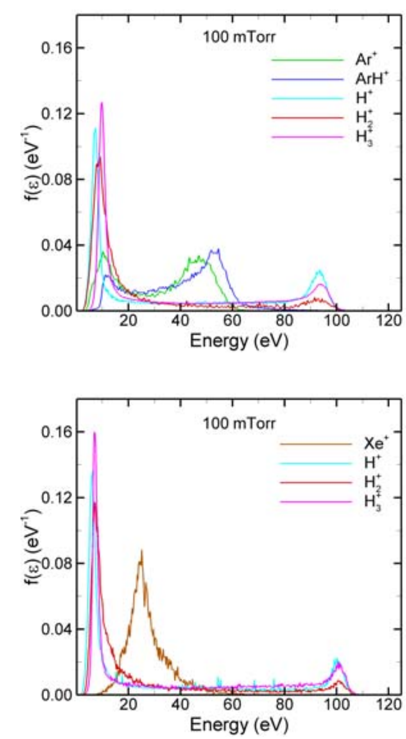

Fig. 1: IEDs for a pulsed dc bias of -100 V with pulse repetition frequency (PRF) of 500 kHz and a duty cycle (DC) of 20% showing separation in energy of high energy peaks between ions having large mass differences. ICP conditions: 30 W (cw), 100 mTorr, 100 sccm. (Left) Ar/H_2. (Right) Xe/H_2.

Work supported by the SRC and the Department of Energy Office of Fusion Energy Science.

1-10

The Role of Micro-Plasmas from Charge Rollers in Printer Engines

Jun-Chieh Wang [a], Seongsik Chang [b], Michael Lee [b], Tom Anthony [b], Napoleon Leoni [b], Henryk Birecki [b], Omer Gila [b], and Mark J. Kushner [a]

(a) Univ. of Michigan, Ann Arbor, MI 48109 USA (junchwan@umich.edu, mjkush@umich.edu)
(b) Hewlett Packard Research Labs, Palo Alto, CA 94304 USA (seongsik.chang@hp.com, michael.lee3@hp.com, tom.anthony@hp.com, napoleon.j.leoni@hp.com, henryk.birecki@hp.com, omer_gila@hp.com)

Conductive charge rollers (CR) are essential components in print engines of, for example, laser printers for surface charging of the cylindrical photoconductor (PC). The charging results from atmospheric plasmas in ambient air produced between the electrically biased CR and the PC. The charging process is essentially a dielectric-barrier-discharge in that the PC behaves like an insulator having a conductivity < 10^{-15} cm^{-1}-Ω^{-1}. If operated with a dc or quasi-dc voltage, the discharge is terminated by surface charging of the PC. The charging process appears to be continuous as the CR and PC surfaces move at speeds of tens to hundreds of cm-s^{-1}. The discharge is re-ignited as the voltage drop between the CR and the incoming uncharged surface of the PC rebounds.

In this study, a multi-dimensional computer model, *nonPDPSIM*, was used to investigate the CR produced microplasmas and the charging process of the PC. *nonPDPSIM* solves transport equations for charged and neutral species, Poisson's equation for electric potential, and the electron energy equation for electron temperature. A Monte Carlo simulation is used to track sheath accelerated secondary electrons and the energy of ions incident onto surfaces. Radiation transport is addressed using Green's function approach. We found that the applied voltage waveform and material properties of CR are important to operation. The uniformity of surface charges on the PC is sensitive to the material properties and speed of the moving surface. A periodic charging pattern due to micro-plasma self-pulsing is computationally reproduced and consistent with experiments. Parametric results for uniformity of charging of the PC will be discussed. For example, the time evolution of electron density and electric potential between the CR and PC are shown in Fig. 1. The PC surface moves from right to left. When the avalanche occurs, a micro-plasma negatively charges the underlying PC, the gap voltage drops and terminates the plasma. Meanwhile, the moving PC translates the surface charges away and brings uncharged surface toward in from the right. When the gap potential between the CR and incoming uncharged surface rebounds, the micro-plasma is re-ignited. A periodic charging pattern is produced.

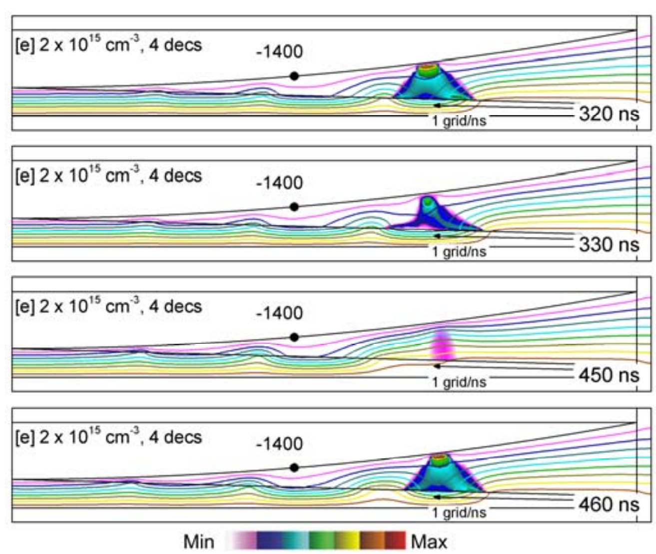

Fig. 1: Electron density (color Flood, cm^{-3}) and electric potential (contour lines, V) with the underlying PC surface rapidly moving from right to left.

Work supported by HP Research Labs.

1-11

Including Convective Flows in a Self-Consistent Hydrogen-Based Microwave PACVD Reactor Model

C. S. Meierbachtol [a], T. A. Grotjohn [a] and B. Shanker [a,b]

(a) Department of Electrical & Computer Engineering, Michigan State University
(b) Department of Physics & Astronomy, Michigan State University
(meierbac@egr.msu.edu)

Microwave Plasma-Assisted Chemical Vapor Deposition (PACVD) reactors are used to deposit diamond films. Recent experiments at higher pressures have resulted in faster diamond growth rates and higher quality samples.[1] However, the reasons for this improvement, and the underlying physics of the deposition process are still not completely understood. Empirical evidence suggests that at higher pressures, convective forces due to the gas flow may affect the plasma discharge, which in turn affects the deposition process. However, measuring these forces is difficult. To aid in the physical understanding and the design of future reactor systems, a self-consistent multi-physics numerical model capable of simulating hydrogen-based plasmas in Microwave PACVD reactors is under development.

The model consists of two major components: 1) a finite difference frequency-domain (FDFD) electromagnetic model, and 2) a steady-state fluid-based plasma model. The plasma module is updated through the conservation of physical quantities. Mass and energy are updated via Gauss-Seidel line relaxation, while the average gas flow is updated via an implicit, pseudo-time stepping backward pressure correction.[2] A single self-consistent solution is ensured by coupling the two modules through the absorbed power density and complex conductivity distributions.

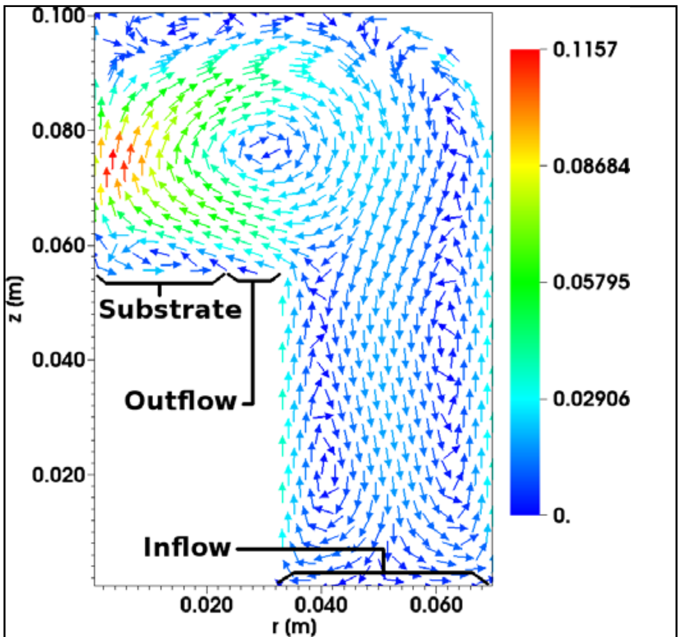

Fig. 1: Average vector flow pattern in the MSU MPACVD Reactor during operation at 200 Torr and 2 kW. The vertical scale is in units of m/s.

Even at the typically low inflow rates, convective forces begin to influence the plasma formation and its location at pressures approaching 150 Torr. These forces effectively lift the plasma off the substrate surface, as well as a redistribute species away from its center. These forces primarily affect the atomic hydrogen mole fraction distribution and location.

Numerical results for various reactor configurations, and operating pressures and powers, will be presented at the time of the conference. The influence of convective forces on numerous plasma properties will also be presented.

References

[1] K. W. Hemawan, T. A. Grotjohn, D. K. Reinhard, J. Asmussen, Diam. Rel. Mater. **19**, 1446 (2010).

[2] G. Strang, *Computational Science and Engineering*, Wellesley-Cambridge (2007).

1-12

Performance Improvement of a Particle-in-Cell Simulation Using GPUs

Seok Won Hwang, In Cheol Song and Hae June Lee

Pusan National University, South Korea (haejune@pusan.ac.kr)

Million time steps are needed to reach a steady state in a conventional plasma discharge simulation or to accelerate an electron beam to the energy of several hundred MeV in a laser-plasma simulation. A graphic processing units (GPU) has several hundred arithmetic logic units (ALUs) and so is adequate to solve problems with a single instruction multiple data (SIMD) algorithm. To improve the performance of PIC simulations using GPUs, particle push algorithms must be parallelized more than all. The Poisson's solver must be also parallelized in plasma discharge simulations. In parallel codes, most of calculation time is allocated at the memory access between GPU processors and GPU memory. Therefore the bottleneck from memory access is an important factor for a performance improvement. To reduce the bottleneck, the information of computer particles is needed to be rearranged in memory. In this work, the methods to reduce the simulation time are suggested, and the performance comparisons are presented.

Functions	CPU (Xeon E5430)	Nehalem i5 750	GTX 260	C1060	SPEEDUP
Move + Sort	76.8 (sec)	75 (sec)	4.5 (sec)	17.9 (sec)	4.2 ~ 17x
Deposit	43.58 (sec)	81(?) (sec)	0.64 (sec)	0.895	48 ~ 68x
Total	120.3 (sec)	156 (sec)	5.43 (sec)	19.2	6 ~ 22x

Fig. 1: Comparison of Performance, GPU vs CPU

Reference

[1] George Stantchev, William Dorland and Nail Gumerov, Journal of Parallel and Distributed Computing **68**, 1339 (2010).

1-13

Characteristics of Radio-Frequency Driven Discharges in Sub-micro Gap

Hyo Won Bae, Seung Bo Shim, In Cheol Song, and Hae June Lee

Department of Electrical Engineering, Pusan National University (hw0417@pusan.ac.kr)

Radio frequency (RF) discharges have advantages in confining the ions in the plasma compared with rectangular pulse discharges because RF period is shorter than the ion transit time. In a plasma display panel (PDP), improving the luminous efficacy has been one of the most important issues to compete other display devices such as liquid crystal displays (LCD) or organic light emitting diode (OLED) displays. Therefore, radio frequency drive was adapted to a plasma display panel in this work. Fluid simulation is performed to investigate the characteristics of RF discharges from 1 MHz to 40 MHz for a conventional PDP structure with 3 electrodes and 80% Ne and 20% Xe composition at 400 Torr. Two kinds of radio frequency driving scheme is used. Spatial density evolution, discharge efficiency, electric power dissipated by electron and ions, and discharge current are observed and analyzed in this work. Highest discharge efficiency was obtained at 1 MHz, which is related to the ion transit time.

References

[1] J. P. Boeuf, J. Phys. D: Appl. Phys. 36, R53 (2003).
[2] H. J. Lee, H. C. Kim, S. S. Yang, and J. K. Lee, Phys. Plasmas 9, 2822 (2002).
[3] I. C. Song, J.-W. Ok, S. W. Hwang, H.-J. Lee, C.-H. Park, D.-K. Lee, and H. J. Lee, Thin Solid Films 518, 3122 (2010).

1-14

Effects of Random Circuit Fabrication Errors on Small Signal Gain and Output Phase in a Traveling Wave Tube

I. M. Rittersdorf [a], T. M. Antonsen, Jr. [b], D. Chernin [c], and Y. Y. Lau [a]

(a) University of Michigan (ianrit@umich.edu)
(b) University of Maryland
(c) Science Applications International Corporation

Traveling-wave tubes (TWTs) are widely used as amplifiers in broadband radar, communications, and electronic warfare [1]. Random fabrication errors in the manufacture of slow wave circuits may have detrimental effects on the performance of traveling-wave tubes of all types. Such errors will pose an increasingly serious problem as TWTs are designed and built to operate in the sub-millimeter wavelength regime, which employ miniature, difficult-to-manufacture slow-wave circuits. As a result of performance degradation from random errors, the manufacturing yield, and therefore the cost of manufacturing, is seriously affected. Analytical and numerical results on the expected degradation of the small signal gain, and the expected output phase variations, of a TWT when small random, axially varying perturbations are present in the circuit phase velocity are obtained (Fig. 1). A scaling law for the ensemble-averaged gain and phase variations is derived. The present work accounts for non-synchronous beam velocities and the inclusion of Pierce's "space charge" effects. In the absence of space charge, analytical results using a perturbative approach and a Ricatti method compare favorably with numerical integration of the governing equation using 500 random samples, in both gain and phase modifications as a result of the errors in the phase velocity that are randomly distributed along the slow wave circuit (Fig. 1). Results on the effects of non-synchronous beam velocities and of ac space charge are reported. Effects of internal reflections are investigated [2]. This work was supported by AFOSR, L-3, Northrop Grumman, and MIPSE.

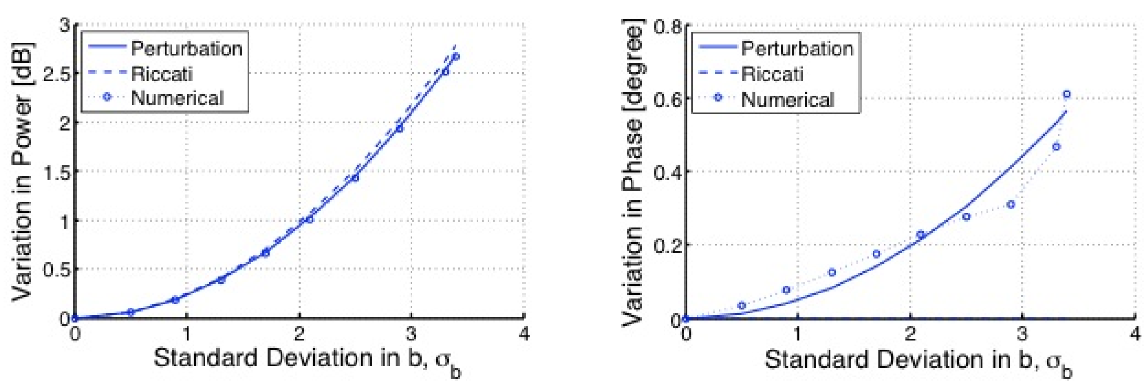

Fig. 1: Mean values of the power (left) and phase (right) phase at a TWT output relative to the unperturbed values, as a function of circuit random errors, from three approaches.

References

[1] P. Pengvanich, D. Chernin, Y. Y. Lau, J. W. Luginsland, and R. M. Gilgenbach, *IEEE Trans. Electron Devices* **55**, 916 (2008); and references therein.

[2] D. Chernin, I. Rittersdorf, Y. Y. Lau, T. M. Antonsen, and B. Levush, *IEEE Trans. Electron Devices* **59**, 1542 (2012).

2-01

Multipactor Suppression in Resonant Cavities via Secondary Modes

Scott A. Rice, John Verboncoeur

Michigan State University (ricesco1@msu.edu, johnv@msu.edu)

Multipactor is a resonant phenomenon in which an electromagnetic field causes a free electron to impact a surface, resulting in the surface emitting one or more secondary electrons. If the surface geometry and electromagnetic fields are appropriately arranged, the secondary electrons can then be accelerated and again impact a surface in the bounding geometry. If the net number of secondary electrons participating in multipactor is non-decreasing, then the process can repeat indefinitely. This phenomenon is of considerable practical interest in the design and operation of radio frequency (RF) resonant structures.

When the secondary electron yield (SEY) of a material is measured as a function of the incident electron kinetic energy, the curve follows a similar shape for many materials. [1] As shown in Figure 1 below, at low incident kinetic energies, the SEY is low. At intermediate energies, the SEY is maximized at an incident kinetic energy which is material-dependent. Finally, the SEY tapers down to zero as the incident kinetic energy further increases. In order for multipactor to be self-sustaining, the SEY averaged over the electron ensemble must be at least unity. As denoted in Figure 1, a secondary electron impact event will likely result in a net increase in electrons if the incident electron energy is between E_{min} and E_{max}, which denote the points at which the SEY curve passes through unity.

This research investigates the feasibility of suppressing multipactor through the use of higher-order cavity modes which will modify the incident kinetic energy of the impacting electrons. Since the SEY is dependent upon the kinetic energy of the incident electron, our goal is modify the impacting electron velocities to reduce the average SEY to less than unity such that multipactor is not sustainable. Preliminary computer simulations are presented which demonstrate this concept in reducing or eliminating multipactor in a coaxial cavity geometry.

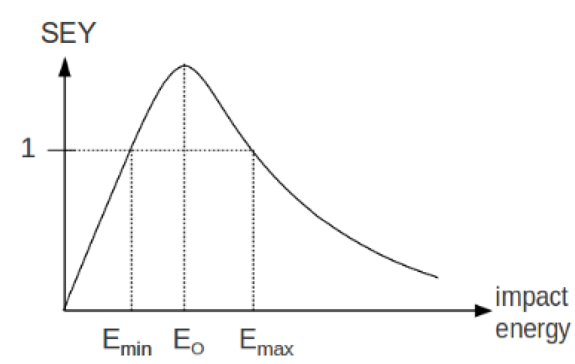

Fig. 1: Typical secondary electron yield (SEY) curve as a function of electron kinetic energy at impact

Reference

[1] CRC Handbook of Chemistry and Physics, 65th Edition, Section 12, p. 115, CRC Press (1994).

2-02

Simulation of Using Background Plasma to Neutralize Charged Particle Thrusters on Nanospacecraft

David Liaw, Thomas Liu, Brian Gilchrist

University of Michigan, Ann Arbor, MI 48109

There is an emerging class of nanospacecraft thrusters under development that use colloids or nanoparticles that can be charged either positively or negatively to provide thrust. An issue to be examined is how to adequately neutralize both the spacecraft and the emitted beam. We initially focused on the capabilities of the nanoparticle field extraction thruster (NanoFET) to self-neutralize (although it applies to colloidal systems as well). The NanoFET system operates by expelling either positively or negatively charged nanoparticles through a gridded structure. This ability to charge nanoparticles to either polarity offers the flexibility to also use the nanoparticles to neutralize the system, which has been previously examined. Most common electric propulsion systems only emit positively-charged ions, which requires that electrons are also emitted, often through the use of hollow cathodes or other electron emitters. These neutralization techniques all reduce efficiency. If NanoFET did not need a separate system to be neutralized, then there would be no loss of efficiency.

Previously, we have explored two approaches for charged particle thruster neutralization: spatially and temporally separated oppositely charged populations of nanoparticles[1]. Both solutions would result in equal amounts of both charged populations being emitted, in theory resulting in a charge neutral spacecraft as well as a net neutral beam. However, in reality, when dealing with such large, heavy, equally "massive" particles of opposite polarities, it is difficult to get them to interact in a relatively short time span and self-neutralize[2]. On the other hand, at the relatively low power levels that a nanospacecraft will be operating at, in the range of 25 W at a 50% duty cycle, it is quite possible that a singly charged beam will be running at a low enough current to provide the propulsion needed as well as be sufficiently neutralized by the ambient space plasma thus negating all detrimental effects of a charged spacecraft and charged beam.

In this presentation, we briefly discuss the NanoFET system, as well as previous attempts to self-neutralize using oppositely charged particles. In addition, there is an in depth analysis, including simulations using OOPIC PRO™, of a singly charged beam being emitted into an ionospheric plasma which neutralizes the emitted beam as well as the spacecraft. We examine at what plasma densities and thus altitudes certain emitted currents will be properly neutralized.

References

[1] Liaw, D. C., Gilchrist, B. E., and Liu, T. M., "Simulation of Self-Neutralization Techniques for Charged Particle Thrusters on Nanospacecraft," *47th AIAA/ASME/SAE/ASEE Joint Propulsion Conference*, San Diego, California, July 31-Aug 3, 2011.

[2] Liaw, D. C., Gilchrist, B. E., and Liu, T. M., "Simulation of Self-Neutralization Techniques for Charged Particle Thrusters on Nanospacecraft," *32nd International Electric Propulsion Conference*, Wiesbaden, Germany, September 11-15, 2011.

2-03

Beryllium Strength under Extreme Dynamic Loading Conditions

Marc Henry de Frahan [a], J. L. Belof [b], R. M. Cavallo [b], O. Ignatova [c], E. Johnsen [a], B. A. Remington [b] and V. Raevsky [c]

(a) University of Michigan (marchdf@umich.edu)
(b) Lawrence Livermore National Laboratory
(c) Russian Federal Nuclear Center – VNIIEF

To achieve ignition, laser inertial confinement fusion (ICF) targets must be uniformly compressed while minimizing the growth of hydrodynamic instabilities that can lead to the introduction of debris into the deuterium-tritium gas. One way to mitigate this mixing is to use an outer shell layer with strength that also has favorable properties for coupling with the x-rays produced by the lasers in the surrounding gold hohlraums. Beryllium (Be) is one such material, but its strength properties are not well understood.

Be strength has been investigated under dynamic loading conditions using platforms that span a limited range of pressure and strain-rate space. Multiple Be strength models persist that are ostensibly calibrated to these experiments. However, they predict different results beyond the limited phase space where data exist. We discuss experiments using high explosives (HE) to accelerate a solid rippled Be target quasi-isentropically. In this experiment, a small HE charge is detonated nearby the Be sample. As the gaseous HE products expand, they accelerate the target. The interface between the low-density gas and the perturbed face of the solid target is Rayleigh-Taylor (RT) unstable, and the amplitude of the ripples will grow with time. The ripple growth is mitigated by the strength of the Be. By measuring and modeling the amplitude growth, we can discriminate among various strength models for Be. Our RT designs extend the pressures up to 50 GPa and the strain-rates near 10^6 s^{-1}. As part of the design process, we analyze existing plate impactor and Taylor anvil experiments using available models. In this poster, we present the results of this analysis as well as the designs and preliminary experimental results from the RT experiments.

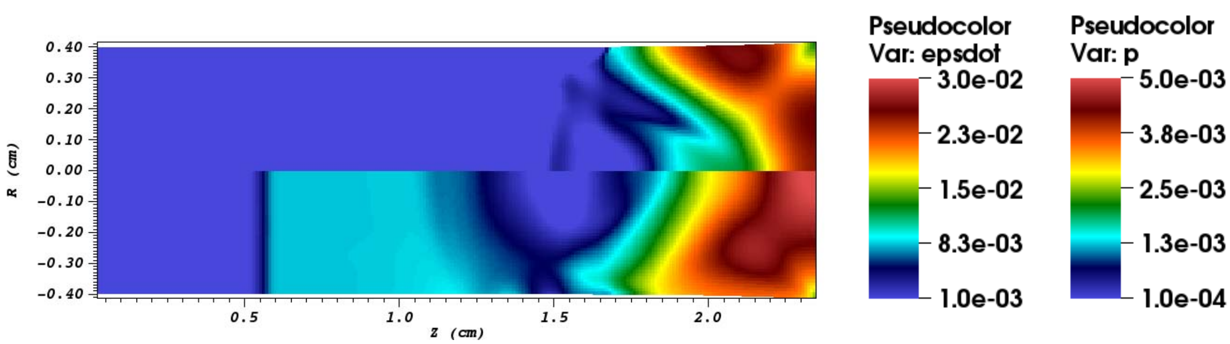

Fig. 1: 2D Taylor anvil simulation with Ares, an ALE hydrodynamics code developed at LLNL. Typical strain-rate (μs^{-1}, top) and pressures (Mbar, bottom) seen in the uniaxial compression of a Beryllium cylinder with impact velocity of 270m/s.

This work was performend under auspices of the Lawrence Livermore National Security, LLC , (LLNS) under contract No. DE-AC52-07NA27344, and under contract No B590737 between LLNL and RFNC-VNIIEF.

2-04

Diffraction of Electron Pulses Generated from Laser-Plasma Wakefield

Zhaohan He [a], Jérôme Faure [b], John Nees [a], Bixue Hou [a], Karl Krushelnick [a] and Alec Thomas [a]

(a) Center for Ultrafast Optical Science, University of Michigan, Ann Arbor, MI 48109 USA
(b) Laboratoire d'Optique Appliquée, ENSTA, CNRS, Ecole Polytechnique, UMR 7639, 91761 Palaiseau, France

Time-resolved electron diffraction is a powerful and rapidly advancing tool for investigating ultrafast structural dynamics in materials with atomic resolution. In conventional ultrafast electron diffraction (UED), electrons from femtosecond laser pulse induced photoemission are accelerated to tens of kilovolts by an external electric field and sub-picosecond temporal resolution has been successfully achieved. It is a challenging task to produce high-brightness electron bunches with a very good temporal resolution (<100 fs) because the Coulomb repulsive space-charge forces in the bunch will inevitably broaden the pulse during propagation. In this study, we report a proof-of-principle experimental demonstration of a novel potential source for UED using electrons generated in plasma wakefield driven by a high-intensity short-pulse laser. The unique phase-space distribution of laser-accelerated electrons has potential advantages in compressibility compared to conventional techniques based on photoemission.

The experiments were performed using the high-repetition-rate λ^3 laser system at the Center for Ultrafast Optical Science of the University of Michigan - a table-top Ti:Sapphire based chirped pulse amplification (CPA) laser capable of delivering pulses with energies up 8 mJ on target and durations of 32 fs at 500 Hz. Electron pulses are generated with quasi-monoenergetic spectrum peaked at 100 keV range by acceleration in slow (non-relativistic) plasma waves on the density downramp of a 100 µm scale argon plasma. The laser pulse is focused by an *f*/2 off-axis parabola to a 2.5 µm (FWHM) spot producing a peak intensity of 3×10^{18}W/cm^2. A deformable mirror is used to optimize the focal spot to maximize the electron flux using a feedback loop from signal of a silicon PIN photodiode. The accelerated electrons propagate through an aperture and a solenoid magnetic lens. The magnetically focused electron profile is shown in Fig. 1(b). Diffraction images are obtained from a thin polycrystalline aluminum sample [Fig. 1(a)]. The number of electrons per focused bunch is estimated to be on the order of 10^4. The calculated electron energy based on kinematic diffraction theory is in agreement to the measured energy spectra. Effect of solenoid alignment will also be discussed for producing diffraction patterns with unique "streaked" feature [1].

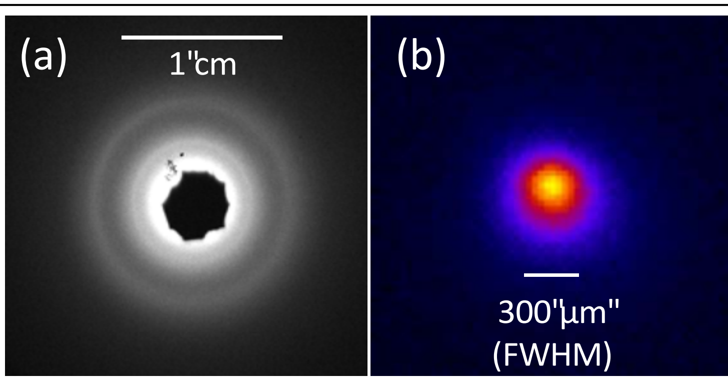

Fig. 1: (a) Electron diffraction pattern of a polycrystalline aluminum foil sample. (b) Image of the focused electron pulse on the scintillator screen without sample.

Reference

[1] E. E. Fill, S. Trushin, R. Bruch, and R. Tommasini, Appl. Phys. B 81, 155 (2005).

2-05

Atmospheric Pressure Microwave-Powered Microplasma Source

P. Liu and T. A. Grotjohn

Electrical and Computer Engineering, Michigan State University, East Lansing, MI 48824 USA

Portable low-cost microplasma sources received great interest in the past decade due to their various applications such as materials processing, biomedical and chemical analysis and optical radiation sources.[1-6] Especially for the atmospheric pressure microwave plasmas without the requirement of vacuum systems, it is possible to realize 3D operations and portable low-cost units. Further, by using higher frequency energy (radio frequency and microwave) to power the microplasma discharge, the erosion of electrodes can be reduced or eliminated.

In this investigation a microwave powered microplasma system based on a double-strip-line structure is developed for the generation of atmospheric pressure plasmas with various feed-gases and feed-gas mixtures. The microplasma system is constructed with the top and bottom copper strip-lines separated by a dielectric material, Teflon. The strip-line structure is powered at one end and the plasma formed at the other end where the two metal strip-lines are brought together to a gap distance that is varied from 50-250 microns. The feed-gas or feed-gas mixture is flowed through a channel in the dielectric such that it exits with the feed-gas flowing between the gap created by the two strip-lines. The gas flow channel in the dielectric is 0.25 mm high by 8 millimeters wide. The flow rate is varied from 600-1200 sccm.

Argon and argon-oxygen microplasma discharges are formed in the gap between the two metal strip-lines. The microwave power used for the argon discharges varies from 2 to 30 Watts. The power density in the argon plasma discharge ranges from 500 to few 1000 W/cm^3. The plasma volume is obtained by photographic images of the discharge. In argon-oxygen plasma, oxygen percentage varied from 2% up to 10%. Optical emission spectroscopy technique was used to identify the existence and variation of concentration of excited oxygen atoms. Oxygen-argon plasmas were also tested to etch single crystal diamond sample with different oxygen percentage concentrations and different input powers (10-25 watts).

References

[1] J. Kim, and K. Terashima, Appl. Phys. Lett. 86 (2005) 191504
[2] J. Kim, M. Katsurai, D. Kim and H. Ohsaki, Appl. Phys. 93 (2008) 191594
[3] K. Ogata and K. Terashima, J. Appl. Phys., 106(2009) 023301
[4] J. Gregorio, L. L. Alves, O. Leroy, and C. Boisse-Laporte, Eur. Phys. J. D., 50(2010) 627
[5] S. Schermer, N. H. Bings, A. M. Bilgic, R. Stonies, E. Voges. J. A. C. Broekaert, Spectrochimica Acta Part B 58 (2003) 1585-1596
[6] U. Engel, A. M. Bilgic, O. Haase, E. Voges, and J. A. C. Broekaert, Anal. Chem. 72(2000) 193

2-06

Neutron Generation Using Ultra-Intense Laser Plasma Interactions

C. Zulick [a], F. Dollar [a], J. Davis [b], V. Chvykov [a], G. Kalintchenko [a], A. Maksimchuk [a], G. M. Petrov [b], A. G. R. Thomas [a], L. Willingale [a], V. Yanovsky [a], and K. Krushelnick [a]

(a) Center for Ultrafast Optical Science, University of Michigan (czulick@umich.edu)
(b) Physics Division, Naval Research Laboratory

The generation of directional neutron beams using laser based acceleration mechanisms offers an alternative means to RF accelerators for the generation of fast neutrons. The primary advantage of laser based techniques is the reduction of the charged particle acceleration distance from meter scale to millimeter scale due to the high electrical fields supported by plasmas. Fast neutron beams can be used for neutron radiography [1], imaging [2], fast neutron therapy [3]. Previous work has investigated neutron generation using $^{2}d(d,n)^{3}He$ reactions in bulk deuterated targets, as well as pitcher-catcher configurations[4], $^{7}Li(p,n)^{7}Be$ reactions[5], and $^{7}Be(d,n)^{8}Be$ reactions [6].

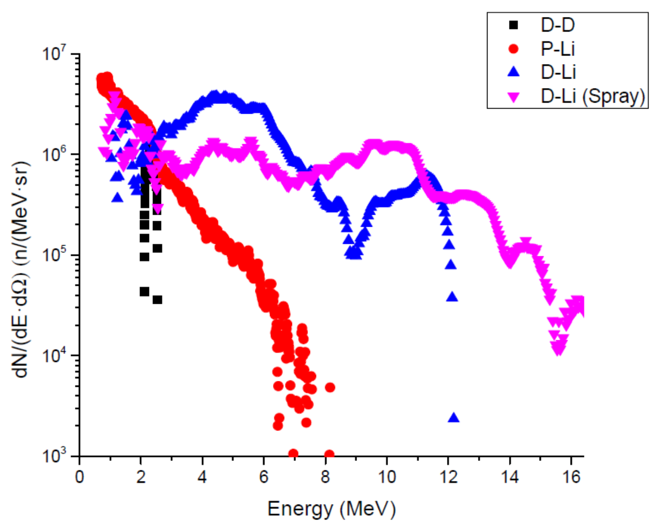

Fig. 1: Experimental spectra from different nuclear reactions (as listed). The D-Li (spray) spectra was from a cryogenically cooled target with frozen D_20.

In this paper, the production of neutrons at ultra-high intensities is reported. Experiments at the HERUCLES laser facility produced neutrons with energies up to 15 MeV in directional beams utilizing $^{2}d(d,n)^{3}He$, $^{7}Li(p,n)^{7}Be$, and $^{7}Li(d,n)^{8}Be$ reactions. The neutrons were produced in a two-stage pitcher-catcher configuration by accelerating protons and deuterons from micron scale solid targets into bulk CD and LiF. A cryogencially cooled target was used to freeze a layer of D20 on the target surface for the D-Li (Spray) target, producing a larger flux of high energy neutrons than deuteron acceleration methods. The neutron yield was measured to be $2.2 \pm 1.2 *10^{7}$ neutrons / sr. A direct comparison to simulation results shows good agreement with experiment.

References

[1] L. J. Perkins, *et.a l.*, Nucl. Fusion **40**, 1 (2000)
[2] M. Borghesi, *et.a l.*, Plasma Phys. Controlled Fusion **43**, 12A (2001)
[3] L. H. Gray, J. Read, Nature (London) **3845**, 53 (1943)
[4] L. Willingale, *et.a l.*,Phys. of Plasmas **18**, 083106 (2011)
[5] K. L. Lancaster, *et.a l.*, Phys. of Plasmas **11**, 7 (2004)
[6] D. P. Higginson, *et.a l.*, Phys. of Plasmas **18** 100703 (2011)

2-07

Plasma Formation inside Deformed Gas Bubbles Submerged in Water

Bradley S. Sommers [a], John E. Foster [b]

(a) Dept. of Nuclear Engineering, University of Michigan, Ann Arbor, USA (bsso@umich.edu)
(b) Dept. of Nuclear Engineering, University of Michigan, Ann Arbor, USA (jefoster@umich.edu)

Plasma formation in liquids produces highly reactive products that have garnered interest for a variety of applications, including water purification and waste processing [1]. The direct ignition of plasma in these environments, however, is limited by the large breakdown strength of these liquids, which imposes severe voltage and energy requirements on the design of practical devices. One way to address this issue is by first igniting plasma in gas bubbles injected into the water. These bubbles provide an environment with higher reduced electric field (E/N) that is more suitable for plasma formation [2]. If such bubbles are be excited into strong distortions of their shape and volume, then it is possible to further enhance E/N, both by field enhancement at the bubble's highly distorted dielectric interface (via E) [3] and by fluctuations in its internal gas pressure (via N).

Bubbles with diameter 0.4-0.7 mm are suspended using a 26.4 kHz underwater acoustic standing wave and excited into nonlinear shape oscillations using an A.C. electric field of amplitude up to 30 kV cm^{-1}. Oscillations of the deformed bubble are photographed with a high speed camera operating up to 30,000 frames s^{-1} and the resulting images are decomposed into their axisymmetric spherical harmonic modes, Y_l^0, using an edge detection algorithm. The electrostatic solver Maxwell is then used to estimate the enhancement of the electric field in cases where the bubble undergoes extreme distortion. Finally, a separate high voltage 1000 ns pulse is applied across the bubbles during different stages of distortion to determine what effect bubble distortion has on the formation of plasma inside the bubble.

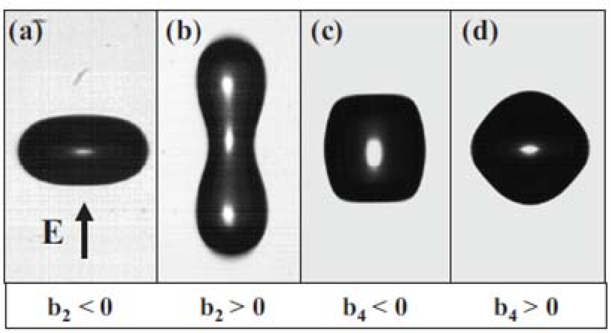

Fig. 1: An underwater gas bubble is distorted into the first two even spherical harmonic modes by an A.C. electric field. Parts (a) and (b) show the L = 2 mode while (c) and (d) show the L = 4 mode.

References

[1] Locke B R, Sato M, Hoffman M R and Chang J S 2006 *Ind. Eng. Chem. Res.* **45** 882-905
[2] Bruggeman P and Leys C 2009 *J. Phys. D* **42** 053001
[3] Stratton J A 1941 *Electromagnetic Theory* (New York: McGraw-Hill) Chp. 3

2-08

Atomic Composition of Diamond-Like Carbon Film Coated at over 100 μm/h by Using Microwave-Excited High-Density Near Plasma

Yasuyuki Takaoka [a], Hiroyuki Kousaka [a], Mashahiro Kawaguchi [b], Noritsugu Umehara [a]
(a) Dept. of Mechanical Science and Eng., Nagoya Univ. (takaoka@ume.mech.nagoya-u.ac.jp)
(b) Tokyo Metropolitan Industrial Technology Research Institute

With increasing demands for energy savings by friction reduction and lifetime extension, the use of DLC (Diamond-Like Carbon) is also increasing. In this field, higher-speed 3-dimensional coating methods are desired. Plasma enhanced CVD (PECVD) is a promising candidate for such applications due to its excellent capability for coating 3-D shapes. However, typical coating speeds of DLC with conventional PECVD are only ~1 μm/h. Further increases in the coating speed are not expected due to the use of low-density (n_e~10^8–10^{10} cm^{-3}) DC or RF plasmas. The use of higher-density plasmas is necessary to increase the coating speed. Thus, we have proposed a high-speed DLC coating method using a novel PECVD having a much higher-density plasma (n_e~10^{11}–10^{13} cm^{-3}) which is sustained by microwave propagation along the plasma-sheath interface on a metal surface [1,2]. In our previous work, DLCs obtained with DC and microwave plasmas were compared [3]. In this work, film properties were investigated from the view point of atomic composition in to understand DLC properties deposited at over 100 μm/h.

Figure 1 shows our experimental apparatus. A base pressure of 1 Pa is obtained before deposition. 2.45-GHz microwaves are injected from a coaxial waveguide connected at the lower flange, propagating into the chamber through a quartz window. A specimen is installed so that the one end contacts the quartz window. In addition, tungsten wiring is connected to the specimen to apply negative voltage from a pulsed DC power supply.

DLC films were deposited by different 3 methods: DC plasma, DC plasma with additional heating, and with microwave-excited plasma. (See Table 1.) The deposition rate and hardness of the DLC deposited by DC plasma were 2.5 μm/h and 11.8 GPa, that for the DLC deposited with the microwave plasma were 156 μm/h and 20.8 GPa. Figure 2 shows the atomic composition of DLCs. Comparing the DC plasma and microwave-added plasmas, both the H and Si content decreased, while the carbon content significantly increased.

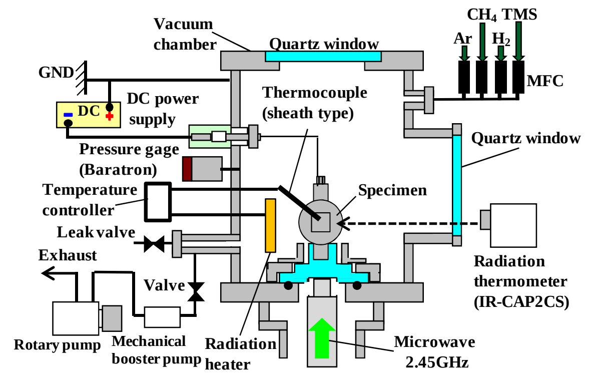

Fig.1: Schematic of DLC coating apparatus with a novel plasma CVD employing high-density near plasma.

Table.1 Coating conditions

		DC	DC+Heater	DC+MW
Gas flow, sccm	Ar	40		
	CH_4	200		
	TMS	20		
Total gas flow Q_{total}, sccm		260		
Pressure P, Pa		75		
Deposition time t, sec.		750	1200	12
Microwave (2.45 GHz)	Peak power			1 kW
	Pulse frequency			500 Hz
Bias	Voltage	-500 V		
	Pulse frequency	500 Hz		
Duty ratio		50%		
Temperature T, °C		80	270	270

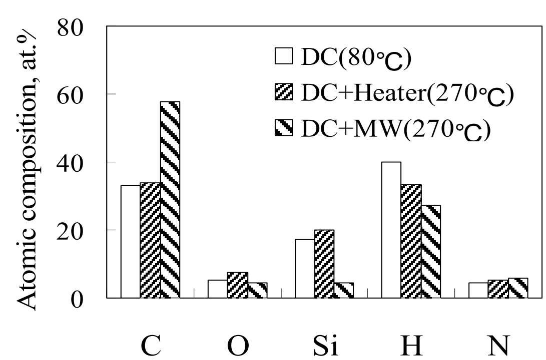

Fig.2: Atomic composition of DLC films deposited by DC plasma, DC with heater and DC with microwave plasma.

Research partly supported by Adaptable & Seamless Technology Transfer Program.

References

[1] H. Kousaka, et. al., *Jpn. J. Appl. Phys.* **44** (2005) L1154–L1157.
[2] H. Kousaka, et. al., *Transactions of the Materials Research Society of Japan*, 31, No. 2 (2006) 487–490.
[3] Y. Takaoka, H. Kousaka, and N. Umehara., Proc. ISPlasma2012, p. 188.

2-09

Quality and Internal Stress of Single Crystalline Diamond Synthesized by Microwave Plasma Assisted Chemical Vapor Deposition

Matthias Muehle [a,b], M. K. Yaran [a], M. F. Becker [a], T. Schuelke [a], J. Asmussen [a,b], Y. Gu [b], D. K. Reinhard [b], T. A. Grotjohn [b]

(a) Fraunhofer USA Inc., Center for Coatings and Laser Applications, East Lansing, MI 48824, USA (mmuehle@fraunhofer.org)

(b) Michigan State University, East Lansing, MI 48824, USA (same as above)

Efficient synthesis of large volume single crystalline diamonds (SCD) is desired for high performance technical and scientific applications such as optics and electronics. Buildup of stress in such crystals during the synthesis process limits achievable sizes and applications. Thus the SCD synthesis process must be optimized to reduce the stress states.

This paper presents initial results of an experimental investigation of SCD properties as a function of synthesis process conditions, resulting impurity levels and defect densities using optical absorption spectroscopy, Raman spectroscopy, birefringence imaging and secondary ion mass spectroscopy (SIMS).

SCD samples were produced by microwave plasma assisted chemical vapor deposition (MWPACVD) at pressures of 160 and 240 Torr. The latter process was developed on a new reactor specifically designed for higher pressure CVD conditions [1]. Data were also compared to high-pressure high-temperature (HPHT) crystals of type Ib, which were acquired from a commercial vendor. These HPHT samples also served as seed crystals for homoepitaxial MWPACVD of new SCD material.

Raman spectroscopy results indicate that the MPACVD SCD samples are of high crystal quality. The full width at half maximum (FWHM) of the Raman signal at 1332 cm^{-1} is generally below 1.60 cm^{-1} at nitrogen impurity concentrations below 0.4 ppm. These FWHM values increased with the nitrogen impurity concentration between 0.3-200 ppm leading to lower crystal quality.

Crystal internal stress values were quantified based on Raman peak shift measurements using an equation from [2]. The as-acquired HPHT crystals had a nitrogen impurity concentration of 200 ppm and an internal stress of 49 MPa. The internal stress in these HPHT crystals was found to have reduced by as much as 50% after they were used for homoepitaxial growth and thus exposed to temperatures on the order of 1200 °C. The nitrogen impurity concentrations in MWPACVD synthesized crystals ranged from 0.4-1.3 ppm depending on growth process conditions. However, internal crystal stress values varied greatly for the MWPACVD diamonds as a function of the synthesis process ranging from 158-207 MPa for the 160 Torr process and 61-73 MPa for the 240 Torr process.

The experiments clearly show the substantial influence of the synthesis process and its dynamics on the stress state of produced SCD crystals. Nitrogen impurity levels directly affect the SCD crystal quality. However, our experiments showed that the higher internal stress levels measured in MWPACVD grown SCD cannot be directly linked to the nitrogen impurity concentration. Therefore other sources such as lattice level defects must be responsible. MWPACVD SCD synthesis at higher pressures and power densities appears to be a promising direction for further process optimization to reduce internal crystal stress.

References

[1] Y. Gu, Diamond and Related Materials **24**, 210 - 214 (2012),

[2] J. Ager, Physical Review B48 **4**, 808-815 (1993)

2-10

Investigating Low Earth Orbit Plasma Interaction to Enhance Understanding of Miniaturized Electrodynamic Tether Propulsion for Femtosatellites and Picosatellites

Iverson Bell, David Liaw, and Brian Gilchrist

The University of Michigan, Ann Arbor, MI 48109 (icbell@umich.edu)

The picosatellite (100 g–1 kg) and femtosatellite (<100 g) system concepts, often referred to as "satellites-on-a-chip", "ChipSats", or "ultra-small satellites", are the next steps in satellite miniaturization. Fleets of coordinated, reconfigurable, ultra-small satellites have potential to enable a unique class of space missions, but the full potential of this concept requires maneuverability and propulsion. Miniature electrodynamic tethers (EDTs) show potential to provide ultra-small satellites with propellantless propulsion.[1–3] The concept utilizes a 1–10 m insulated tether and a pair of nearly identical pico- or femtosatellites capable of harvesting solar energy, storing electrical power, and collecting and emitting electrons. Electrons are collected on the surface of a satellite located at one end of the tether and emitted from a satellite located at the opposite end of the tether. The current conducted along the tether interacts with the planetary magnetic field to produce a thrusting force.

In order to evaluate the feasibility of the ultra-small satellite EDT concept, it is important to understand how efficiently electrons can be collected by the anode and emitted by the cathode. Previous research has demonstrated that the efficiency of the tether–plasma interface for current collection and emission is often the limiting factor in the overall EDT system efficiency.[4] Investigating electron emission is critical because the electrons emitted from the cathode may create a barrier for additional emitted electrons. As a result, there is a maximum space charge limited current density that can be achieved at a given bias. We would like to present our analysis on electron emission to ensure that we are below the space charge limit. Furthermore, a model predicting the expected collected anode current has not been identified because of the non-standard geometries of the anode. A variety of simplifying assumptions have been made in previous trade studies to facilitate estimating this current using simple geometry models.[1-3] Our goal is to improve our anode current collection estimate by conducting ground-based plasma experiments that capture critical characteristics of the LEO environment. The experimental design is presented here.

By further investigating the electron emission and collection of the system concept, we aim to gain insight into the feasibility of the dual ultra-small satellite-EDT propulsion concept.

References

[1] I.C. Bell, Spacecraft Charging and Technology Conference. (2010).
[2] I.C. Bell, Gilchrist, B., McTernan, J.K., Bilén, S.G., Voronka, N., Hoyt, R., and Peck, M. IEPC-2011-054. (2011).
[3] I.C. Bell, Gilchrist, B., McTernan, J.K., Bilén, S.G., Voronka, N., Hoyt, R., and Peck, M. AIAA-2011-7322. (2011).
[4] J. McTernan. M.S. Thesis, Aerospace Engineering, Pennsylvania State Univ. (2011).

2-11

Ion Energy Angular Phase Distribution from the Bulk Plasma through Sheath in Single- and Dual-Frequency Capacitively Coupled Plasma

Yiting Zhang and Mark J. Kushner
Electrical and Computer Science Engineering, University of Michigan, Ann Arbor, MI 48109
(yitingz@umich.edu; mjkush@umich.edu)

Process plasmas are utilized in the microelectronics industry for anisotropic etching and deposition through ion energy acceleration in the sheath region. The control of ion energy and angular distributions (IEADs) is of critical importance for anisotropic etching or conformal deposition in microelectronics fabrication. With single frequency capacitively coupled plasmas (CCPs), the narrowing in angle and spread in energy of ions as they cross the sheath are well definable functions of frequency sheath width and mean free path. Dual-frequency capacitively coupled plasmas (CCPs) are being investigated with the goal of having flexible control where the high frequency (HF) controls the plasma density, while the ion energy is mainly determined by the low frequency (LF). However, over select ranges of LF and HF, the IEAD has characteristics of both the LF and HF.

To help understand the influence of both high and low frequencies on IEADs, we report on results of a numerical investigation of phase and spatially resolved transport of ions through the sheath. These results were generated using a two-dimensional plasma hydrodynamics model having an ion Monte Carlo simulation. Inductively coupled plasmas (ICPs) sustained in Ar/$O_2$with a multi-frequency bias on the substrate were modeled. The IEADs are tracked as a function of height above the substrate and phase within the rf cycle. (See Fig. 1.) The computed results are compared to laser-induced fluorescence (LIF) experiments.[1] We found that the ratios of HF/LF voltage and driving frequency are critical parameters in determining the shape of the IEADs, with evidence of the HF component occurring up to 30 MHz. This tunability may provide additional control for the width and maximum energy of the IEADs.

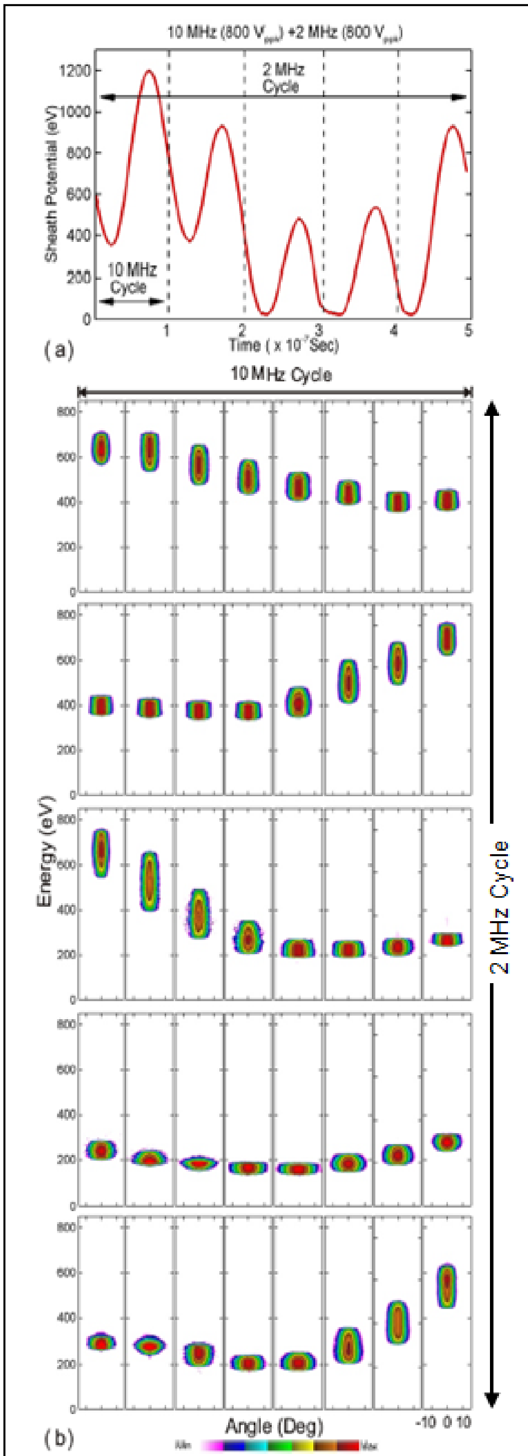

Fig. 1: IEADs for an ICP sustained in Ar/ O_2=80/20, 2 mTorr, LF=2 MHz, 800 V_{ppk} and HF=10 MHz, 800 V_{ppk}. (a) Amplitude of sheath potential during one 2 MHz period. Dash lines mark the 10 MHz period, and each column corresponds to each row below. (b) IEADs of Ar^+ at the middle of the wafer divided by forty phase bins. The phases refer to LF.

Reference

[1] B. Jacobs, W. Gekelman, P. Pribyl, and M. Barnes, Phys. Rev. Lett.**105**, 075001 (2010)

2-12

Space Charge Compensation Measurements of Multi-Charged Ion Beams Extracted from an ECR Ion Source

Daniel Winklehner, Daniela Leitner, Guillaume Machicoane, Dallas Cole, Larry Tobos

National Superconducting Cyclotron Laboratory, Michigan State University, 640 S Shaw Lane, East Lansing, MI 48910, USA

Space charge compensation in beam lines due to the interaction of the beam with residual gas molecules is a well-known phenomenon for high current injector beam lines. When the beam interacts with the residual gas in the beam line, electrons are separated from gas molecules and accumulate inside the beam envelope, thereby compensating the space-charge (neutralization). For beam lines using mostly magnetic focusing elements and for pressure above 1E-6 mbar, neutralization up to 99% has been predicted [1] and observed [2]. However, due to the low pressure required for the efficient transport of high charge state ions, ion beams in ECR injector lines are typically only partly neutralized and space charge effects are present. With the dramatic performance increase of the next generation Electron Cyclotron Resonance Ion Sources (ECRIS) it is possible to extract tens of mA of beams from ECR plasmas. In this high current regime, non-linear focusing effects due to the space-charge potential of the beam become more and more important. In order to develop a realistic simulation model for low energy beam transport lines, it is important to estimate the degree of space charge compensation. In this contribution we report on measurements of the beam potential performed after the extraction region of the ECR ion source in dependence of the base pressure in the beam line and other source parameters using a Retarding Field Analyzer (RFA). If the beam current is known, it is possible to infer the level of neutralization from the measured beam potential. Results are discussed and compared to simulations.

References

[1] I. A. Soloshenko, Rev. Sci. Instrum. **67**(4), 1646 (1996).
[2] R. Ferdinand et al., PAC'97 (1997).

2-13

Similarities and Differences in Low-to-Mid Latitude Geomagnetic Indices during Storms

Roxanne M Katus, Michael W. Liemohn

Atmospheric, Oceanic and Space Science, University of Michigan, Ann Arbor, MI, United States

Several versions of low-to-middle latitude geomagnetic indices are examined with respect to a normalized timeline based on several key storm features. In particular, we examine the well-known Dst and SYM-H indices, as well as a few other more recently-developed storm-intensity indices. These superposed indices are quantitatively compared, using the bootstrap method to quantify the error analysis, and employing descriptive statistics and significance tests to assess the similarities and differences between them. The results are then categorized by storm intensity, storm phase, and solar wind driver. While the indices are highly correlated with each other, dramatic deviation between the indices exists at certain storm epoch times and for certain types of magnetic storms. In particular, the correlation degrades at storm peak and especially for more intense storms. These indices are compared against simulation results from the Hot Electron and Ion Drift Integrator (HEIDI) model, which has been run for every intense storm from the last solar cycle with several input and boundary condition settings. Current systems and magnetic perturbations from these simulation results, which are also scaled onto a normalized storm-based timeline and categorized by storm intensity, storm phase, and solar wind driver, are used to interpret the physical processes underlying the systematic differences in the various ground-based magnetometer indices.

2-14

Lacunae-Based Stabilization of FDTD Mesh Refinement

Eric Wolf, Andrew Christlieb

Department of Mathematics, Michigan State University (wolferi1@msu.edu, christlieb@math.msu.edu)

The ability to use multiple mesh sizes in a single simulation allows one to resolve features at multiple scales at a much lower cost than when using a uniform mesh size dictated by the smallest scale present in the simulation. The technique of mesh refinement (often called subgridding in the finite-difference time domain (FDTD) literature) places a fine mesh in the regions where small-scale features need to be resolved, and a coarse mesh where there are no small-scale features or where they need not be resolved. The partition of the mesh into coarse and fine regions may be done *a priori* before the simulation is run or *a posteriori* as the simulation is run, as in adaptive mesh refinement (AMR). The application of mesh refinement to electromagnetic particle-in-cell (PIC) simulations of plasmas [1] depends upon the success of the application of that technique to the FDTD simulation of Maxwell's equations.

Many mesh refinement schemes have been proposed for FDTD, and all have to deal with the problem of the potential reflection of high frequency waves at the fine-coarse mesh interface. Berenger [2] has recently proposed a scheme in which communication between fine and coarse meshes is done through equivalent sources. This results, however, in a late-time instability due to the mishandling of high frequency content. In this work, we investigate a possible remedy for this instability, using the lacunae-based mesh truncation [3] in a 1D test problem for the scalar wave equation.

References

[1] J.-L. Vay, P. Colella, P. McCorquodale, B. Van Straalen, A. Friedman, and D.P. Grote, Laser Part. Beams **20**, 569 (2002).

[2] J.P. Berenger, IEEE Trans. On Ant. And Prop. **54**, No. 12, (2006).

[3] S.V. Petropavlovsky, S.V. Tsynkov, J. Comp. Phys. **231**, (2011).

3-01

Investigation of EEPFs in a Micro Dielectric Barrier Discharge at Atmospheric Pressure Using a Particle-in-Cell Simulation

Jung Yeol Lee [a], Hyo Won Bae [a], John Verboncoeur [b], and Hae June Lee [a]

(a) Pusan National University, Busan. South Korea (leejungyel@naver.com, dreamdol2@gmail.com)
(b) Michigan State University (johnv@msu.edu)

Recently, atmospheric pressure micro plasmas attract lots of interests for the useful applications such as surface modification and bio-medical treatment. Among many plasma devices, a dielectric barrier discharge (DBD) is conventionally used for the simplest device which can sustain glow discharge with a short gap length. However, experimental diagnostics of micro DBDs are limited for spatio-temporal analysis of the discharge. In this study, a particle-in-cell Monte Carlo collision (PIC-MCC) simulation was adopted to compare the discharge characteristics of a planar micro DBD with a driving frequency from 13.56 MHz to 162.72 MHz with different heating modes, the alpha and the gamma mode.[1][2] In a gamma mode where the secondary electron emission plays an important role in sheath heating, the electron energy distribution function (EEDF) shows two-temperature profiles. The variation of frequency results in the change in the electron density through the relationship between the ion transit time and the driving period. On the other hand, ohmic heating is more dominant in alpha mode. It is possible to categorize the efficient operation range of DBDs for its applications by controlling the interactions between plasmas and neutral gas for the generation of preferable radicals. Finally, the variation of ion fluxes at the dielectric surface induces heating mode transition of atmospheric dielectric barrier discharges.

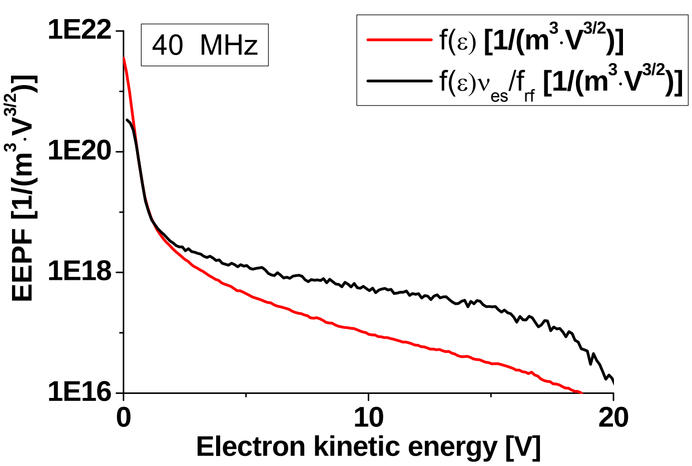

References

[1] V. A. Godyak et al., Phys. Rev. Lett. 65, 996 (1990).
[2] V. A. Godyak et al., Phys. Rev. Lett. 68, 40 (1992).

3-02

Stimulated Beam Extraction Performance Characterization of a 50-cm Ion Thruster Discharge

Pietro Ranieri [a], John Foster [a], Chris Davis [b], Eric Viges [b]

(a) University of Michigan (pranieri3@gmail.com, jefoster@umich.edu)
(b) EDA (davis@edapplications.com, viges@edapplications.com)

The 50-cm ion thruster is being developed to address the gap of near-earth operations between current ion thrusters and next generation electric propulsion that require a range of thrust-to-power. The most advanced ion thruster thus far is embedded in the NEXT ion thruster. This thruster can process up to 7 kW; however the near future needs of space propulsion will require a single, high TRL level gridded ion thruster with input power greater than 10 kW. [1] The 50-cm ion thruster is designed to push this 7 kW power input up to 25 kW. The thruster will use next generation thin film solar arrays as a power source to combine both the efficiency of the ion thruster with the renewable energy of the solar arrays; thus enabling more missions for satellites. [2] The goal parameters for the 50-cm ion thruster is to operate at >65% efficiency at 11 kW and 2700 Isp and >75% efficiency at 25 kW and 4500 Isp. Three technological areas need to be advanced to achieve these results; namely the discharge chamber magnetic circuit, the cathode and neutralizer and the high perveance 50-cm ion optics.

This study investigated the operating characteristics under simulated beam extraction at a range of operating points. The ion thruster has a smaller cylindrical section that expands into a conical section; a change from the total cylindrical shape to reduce mass. The magnetic circuit is optimized within the conical section to be 6 rings of magnets in order to have a field minimum along the axis. A set of 50-cm ion optics have been developed by NASA from a previous study by Patterson. [3] The simulated beam extraction tests were conducted in the LVTF at PEPL. There were two methods of testing, one was to vary the flow with a fixed discharge while the second was to vary the main/cathode flow and discharge current at fixed simulated current. The findings of the previous work on the 50-cm thruster found roughly 80% flatness in the beam uniformity across the outlet of the thruster at certain operating points. The measurement device was a grid with 25 button probes in a line across the diameter of the thruster outlet that measured the overall current density profile and the probes were spaced 2mm apart. By averaging over the 25 button probes, the average beam density can be calculated. This study will explore the different thrust characteristics over multiple operating points to determine beam stability and the beam profile downstream. These findings will be reported as well as future work determined by the study.

References

[1] Patterson, M.J., Pinero, L., and Sovey, J.S., "Near-Term High Power Ion Propulsion Options for Earth-Orbital Applications." Proceedings of the 45th Joint Propulsion Conference, AIAA Paper 2009,-4819, 2009.
[2] "Boeing moving FAST on Satellite Power and Propulsion System," Defense Industry Daily, June 14, 2009.
[3] Patterson, M.J., Roman, R.F., and Foster, J.E., "Ion Engine Development for Interstellar Precursor Missions," AIAA 2000-3811.

3-03

Magnetic Reconnection in Plasma under Inertial Confinement Fusion Conditions Driven by Heat Flux Effects in Ohm's Law

A.S. Joglekar [a], A.G.R. Thomas [a], W. Fox [b], and Amitava Bhattacharjee [b]

(a) University of Michigan – Center for Ultrafast Optical Sciences (archisj@umich.edu; agrt@umich.edu)

(b) University of New Hampshire (willfox@artemis.sr.unh.edu; amitava.bhattacharjee@unh.edu)

In the interaction of high power laser beams with solid density plasma, there are a number of generating mechanisms that result in very strong magnetic fields. Such fields can subsequently inhibit or redirect energy transport. Here, we present 2D numerical modeling of near critical density plasma using a fully implicit Vlasov-Fokker-Planck code, IMPACTA, which includes self-consistent magnetic fields as well as anisotropic electron pressure terms in the expansion of the distribution function. Magnetic field generation and advection by different mechanisms are studied in the context of heating by multiple laser spots, between which reconnection of magnetic field lines may occur. In particular, we compare the relative importance of Hall, resistivity, and heat flux effects in the magnetic field dynamics of MG strength, oppositely aligned magnetic fields interacting in a plasma under conditions relevant to the wall of a hohlraum.

3-04

Directional, Energetic Neutron Generation via High-Intensity Laser/Plasma Interactions at CUOS

Anthony Raymond [a], Anatoly Maksimchuk [a], Vladimir Chvykov [a], Franklin Dollar [a], Louise Willingale [a], Victor Yanovsky [a], Fan Yu [a], Calvin Zulick [a], Karl Krushelnick [a], Jack Davis [b], and George Petrov [b]

(a) CUOS, University of Michigan, Ann Arbor, MI 48109
(b) Plasma Physics Division, NRL, Washington, DC 20375

High-intensity laser/plasma interactions can generate beams of ions that subsequently may be used to produce sources of directional, energetic neutrons.

Pitcher-catcher arrangements were utilized for neutron production via the interaction of a beam of deuterons with catchers materials using the reactions 7Li(p,n) (Q=-1.64MeV), d(d,n) (Q=3.27MeV), and 7Li(d,n) (Q=15.03 MeV). The experiments were conducted at the University of Michigan in Ann Arbor, on both the T-cubed laser system (400fs pulses at 20TW and a focused intensity of $2.6\text{x}10^{19}$ W cm^{-2}), and on the Hercules laser system (40fs at 150TW and $3\text{x}10^{21}$ W cm^{-2}).

The method of deuteron-beam production utilized in the experiments currently described involved the deposition of deuterium oxide onto cryogenically cooled foils of various thicknesses and compositions, which at optimal temporal and volumetric parameters produced deuteron yields substantially greater than that observed in previous experiments [1] involving instead a pitcher target of deuterated-polystyrene (CD) coated 13μm Mylar, as the latter method was shown to be impaired by the effects of hydrocarbon contamination. We present results in which the more recent deuteron-production technique is utilized, which for d-d reactions yielded on the T-cubed system neutrons up to ~2.5 MeV and on the Hercules system up to ~12 MeV, with an average yield in the forward direction on the order of 10^5 neutrons/steradian (being an order of magnitude higher than the flux previously achieved using either a CD coated pitcher target or a bulk target comprised of deuterated polyethylene).

The Office of Naval Research funded this work.

Reference

[1] L. Willingale et al., Phys. Plasmas 18, 083106 (2011).

3-05

X-Pinch Experiments on UM Linear Transformer Drivers

S.G. Patel, D.A. Chalenski, R.M Gilgenbach, A.M. Steiner, D. Yager-Elorriaga, and Y.Y. Lau

Plasma, Pulsed Power and Microwave Lab, Nuclear Engineering and Radiological Sciences Dept.
University of Michigan

The Magneto-Rayleigh–Taylor (MRT) instability is currently being studied at the University of Michigan MAIZE facility. MRT occurs in plasmas in which a light fluid, in this case a magnetic field, compresses or accelerates a heavier fluid. This effect is particularly important to magnetized target fusion in which a cylindrical liner is magnetically compressed and adiabatically compresses a laser created plasma.

The MAIZE Linear Transformer Driver (LTD) can supply 1 MA, 100 kV pulses with a 100 ns risetime into a matched load. Currently, a 400 nm foil is centered between two current return electrodes spaced approximately 1 cm apart. Initially, during the early current rise, the foil ablates. As the current increases the JxB force increases and slows the expansion, resulting in a deceleration toward the middle of the foil. Consequently, MRT forms on both sides of the foil as the magnetic field accelerates the foil plasma. Laser shadowgraphy in the direction perpendicular to the current has already been used to image the foil plasma and characterize the growth rate. [1]

In addition to laser shadowgraphy, hybrid x-pinches [2] have been tested in the MAIZE facility. The x-pinch consists of a single wire separated by conical electrodes between two current return plates. The LTD was charged to +/-70 kV resulting in approximately 0.4-0.5 MA passing through the wire. Initial tests with Mo and Al wires show several x-ray bursts over the length of the current pulse, as shown in Figure 1.

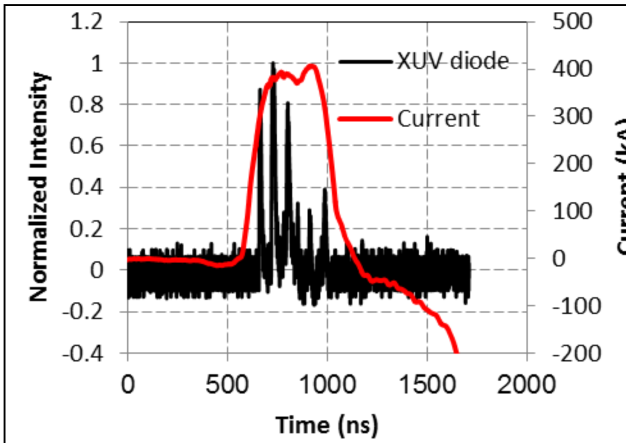

Fig. 1: X-ray burst from a Mo Wire at a peak current of 400 kA.

The x-pinch is expected to be placed in parallel with the 400 nm foil. Through inductive current division, the x-pinch will act as a backlighter for the planar MRT instability, allowing x-ray probing of the foil plasma at higher densities than shadowgraphy would allow.

This work was supported by DoE award number DE-SC0002590, NSF grant number PHY 0903340, and US DoE through Sandia National Labs award numbers 240985 and 76822 to the U of Michigan.

References

[1] J.C. Zier, et al., Phys. Plasmas, 19, 032701(2012).
[2] T. A. Shelkovenko, et al., Phys. Plasmas, 17, 112707(2010)

3-06

A Description of the Experimental Microwave Discharge Behavior versus Pressure, Power and Reactor Geometry for MPACVD Diamond Synthesis Reactors

Jing Lu [a], Yajun Gu [a] and Jes Asmussen [a,b]

(a) Michigan State University, Department of Electrical & Computer Engineering, East Lansing, MI 48824 USA (lujing1@msu.edu)

(b) Fraunhofer USA, Center for Coatings and Laser Applications, East Lansing, MI 48824 USA

Recently two new microwave plasma-assisted chemical vapor deposition (MPACVD) diamond synthesis reactors [1,2] were designed, built and experimentally evaluated, and their performance was compared to earlier MPACVD reactor designs [3]. In order to take advantage of the improved CVD diamond synthesis conditions that occur within the high pressure regime (160-300 Torr) the two reactors were designed to operate with high power densities and at high pressures. When these reactors operate at high pressures single crystal MPACVD diamond synthesis occurs over a large range of reactor conditions [1,2] such as: (1) pressure, p, 100-300 Torr. (2) input power 1-6 kW, (3) flow rates, (4) methane to hydrogen concentrations of < 1% to greater than 9%, (5) discharge power densities of 200-1000 W/cm^3, (6) substrate holder design/geometry, (7) reactor design/geometry and (8) plasma/substrate position, Z_S. During MPCVD diamond synthesis the microwave discharge supplies both the growth species and thermal energy to the substrate. The design, operation and optimization of these MPACVD reactors is a new, complex, and challenging multivariable problem. It is important to develop an experimental understanding of the behavior of the microwave discharge versus pressure and input power, and to understand the variation of diamond synthesis rates versus reactor design.

Here within the 160-300 Torr pressure regime we measure the experimental reactor behavior of several MPACVD designs over the large multidimensional input, internal and output diamond synthesis variable space, and thereby determine their detailed operational performance. An example of such an experimental “operational roadmap” is shown in Fig. 1. Using these measurements the safe and efficient reactor operating conditions that also synthesize diamond and allow the robust long-term reactor operation are identified, in Fig. 1 as the region enclosed by the green dashed lines. This set of curves defines the nonlinear relationships between the reactor’s important internal variables such as substrate temperature, and the input variables like absorbed power and pressure. These measurements enable the calculation of reactor coupling efficiency and provide insight into further improvements in reactor design and performance. Examples of high rate single crystal diamond synthesis achieved inside the efficient operating regime will also be presented and the output single crystal diamond quality will be briefly reviewed.

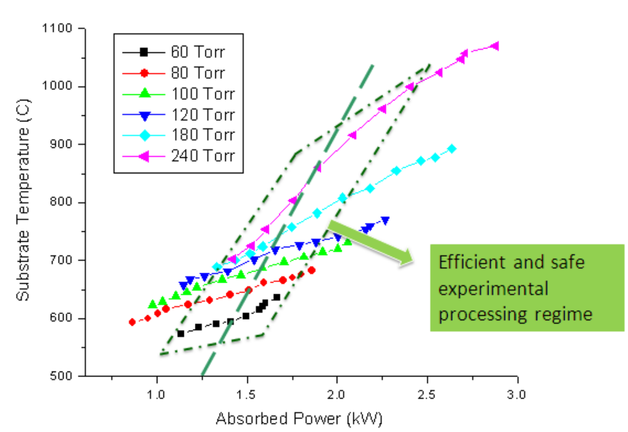

Fig. 1: Experimentally measured reactor operating roadmap curves.

References

[1] K.W. Hemawan et al., Diamond and Related Materials, 19, 1446 (2010).

[2] Y. Gu et al., Diamond and Related Materials, 24, 210 (2012).

[3] K. P. Kuo et al., Diamond and Related Materials, 6, 1097(1997).

3-07

Simulations of Plasma Dynamics of Electrical Discharges Sustained in Bubbles in Water

Wei Tian [a], Mark J. Kushner [b]

(a) Dept. of Nuclear Engr.& Radiological Science, University of Michigan, Ann Arbor, MI 48109, USA (bucktian@umich.edu)

(b) Dept. of Electrical Engr. & Computer Science, University of Michigan, Ann Arbor, MI 48109, USA (mjkush@umich.edu)

Electrical discharges in bubbles in water are being investigated due to their ability to produce chemically reactive species such as hydroxyl and oxygen radicals for applications ranging from environmental cleanup to chemical processing. Due to the large dielectric constant of water ($\varepsilon_r \approx 80$) compared to atmospheric pressure gases, pulsed plasmas in bubbles tend to propagate along the gas-water interface. These plasma dynamics concentrate the plasma power at the location where the water vapor density is highest and so the production of oxidizing radicals is largest. In this paper, we report on a computational investigation of the plasma dynamics in bubbles in water with the goal of quantifying the basic processes. Synthesized images and optical spectra from the bubbles are compared to recent experiments by Tachibana et al.[1]

Discharges in water were simulated for He, Ar and N_2 filled bubbles. Comparisons of results from the model to experiments are shown in Fig. 1. For N_2 bubbles, the discharge is strongly confined to the gas-water interface, while the discharge penetrates into the volume of the bubble to a greater extent when sustained in He or Ar. In N_2, the lower threshold energies for inelastic electron collisions result in an electron temperature that is generally lower and an energy relaxation length that is usually shorter, thereby restricting the discharge to regions having the highest electric fields. These electric fields are are near the boundaries of the bubbles. In He or Ar bubbles, the electron temperature is higher and energy relaxation length is longer, so plasma can be formed over a larger volume of the bubble, even at the lower electric fields near the center of the bubble. These trends are all in good agreement with the experiments.[1] Further investigations will address the use of discharges in bubbles for production of oxidizing radicals for elimination of toxins from water.

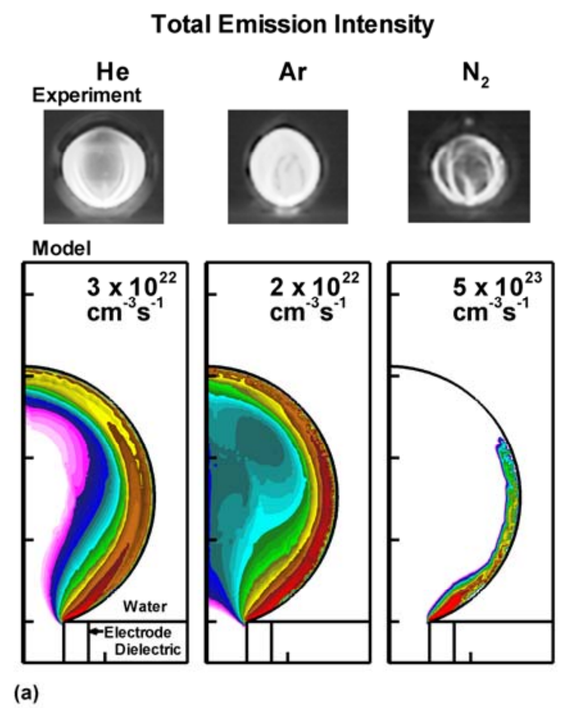

Fig. 1: Images of optical emission from discharges sustained in bubbles of He, Ar and N_2, 1.5 mm in diameter. (top row) Images from the experiments by Tachibana et al.[1] (bottom row) Contours of emission intensity ($cm^{-3}s^{-1}$) predicted by the model (3 decade log scale). Maximum values are shown in each frame.

Reference

[1] K. Tachibana, Y. Takekata, Y. Mizumoto, H. Motomura and M. Jinno, *Plasma Sources Sci. Technol.* **20,** 034005 (2011).

3-08

Kinetic Modeling of Electronically Enhanced Reaction Pathways in Plasma Assisted Combustion

Guy Parsey, Yaman Güçlü and John Verboncoeur

Michigan State University (parseygu@msu.edu, yguclu@msu.edu, johnv@msu.edu)

Plasma Assisted Combustion (PAC) is the concept of using plasmas to manipulate chemical combustion characteristics, such as augmenting efficiency, operating conditions and/or ignition delay. The use of (nearly-) equilibrium plasmas, in the form of arcs or sparks, for thermally initiating reaction chain propagation in the combustion process is well understood and diversely implemented, whereas applications using non-equilibrium plasma discharges are still exploratory. The use of non-equilibrium plasmas within a gas provides a means to excite gaseous species to excited and ionized levels, as opposed to most absorbed energy going into ohmic heating and vibrational levels, altering branched chain combustion mechanisms. Though there exists a plethora of non-equilibrium plasma discharge types and power sources, this work focuses on simulation of direct coupling of electromagnetic power to a combustion region with a low-power microwave source, so as to eventually match experimental efforts being done at Michigan State University.

A modular, numerical and symbolic, python framework is being developed, centered around a kinetic global (volume-averaged) model (KGM) to systematically explore scaling laws in parameter space. Reaction rates are calculated with an optimized electron energy distribution function (EEDF) parameterized with a shaping parameter *x*. Usage of reaction cross section data is limited to open-source databases (e.g. GENIE [1] and LXcat [2]), however this provides a method for comparing numerically computed cross sections and determining data availability limitations. By design, the framework provides a benchmarking tool for understanding the consistency of 'standard' global models and the effect of different computational methods with respect to the sparse, stiff, non-linear system inherent in non-equilibrium PAC (NEPAC).

We first reproduce models presented in other works for validation of our framework and then to study the effect of limiting assumptions; such as a fixed EEDF or non-realistic power coupling. Though a self-consistent solution of the EEDF would require solving the Boltzmann equation, the assumption that the EEDF is a fixed Maxwell-Boltzmann distribution was historically often used in global models and has been numerically shown to be invalid [3]. We then explore theoretical applications of coupling a KGM with a collisional-radiative atomic model (CRM) for self-consistent evaluation of species temperatures dependent on the EEDF. The implementation of a CRM would allow for further model verification by comparing simulation results with spectroscopic measurements of emission lines from related experimental research.

Supported by AFOSR and a Michigan State University Strategic Partnership Grant

References

[1] GENIE: Atomic Data Search Engine. Nuclear Data Section. IAEA. < http://www-amdis.iaea.org/GENIE/>

[2] LXcat. Plasma Data Exchange Project. LAPLACE < http://www.lxcat.laplace.univ-tlse.fr/>

[3] S.K. Nam and J.P. Verboncoeur, Comp. Phys. Comm. **180**, 628-635 (2009).

3-09

Controlling Ion and UV/VUV Photon Fluxes in Pulsed Low Pressure Inductively Coupled Plasmas for Materials Processing

Peng Tian, Mark J. Kushner

Dept. of Electrical Engineering and Computer Science, University of Michigan, Ann Arbor, MI, 48109, USA
(tianpeng@umich.edu, mjkush@umich.edu)

Low pressure plasmas are widely used to modify the surface properties of materials. This is accomplished through a sequence of surface reactions which is initiated by fluxes of reactive species, including electrons, ions, excited neutrals and photons. In particular, UV and VUV photons are increasingly being recognized as being important in surface processes. It has been found that synergistic interactions between ion and UV/VUV photon fluxes may produce undesirable reactions at and below the material surface. These observations have motivated the development of methods to separately control ion and UV/VUV photon fluxes, or at least to control their relative fluxes. Pulsed plasmas are promising for this purpose because ion and photon fluxes respond to pulsed power deposition at different rates.

In this project, pulsed inductively coupled plasmas (ICPs) were computationally investigated as a mean to control relative fluxes (or flux ratios) of ions and photons to substrates in material processing reactors. The pulsed ICPs are generated by application of radio frequency (RF) power to a planar antenna. The RF power is square-wave modulated with varying pulse repetition frequency and duty cycle and fixed average power in each pulse period. The computational platform is a 2-dimensional hydrodynamics model with radiation transport addressed by a spectrally resolved Monte Carlo simulation. We investigated plasmas in Ar/Cl_2 gas mixtures at low pressure (10's of mTorr) using a 20 μs pulse period. It was found that due to the overshoot in electron temperature that occurs at the start of the pulse-on period at low-duty cycle, larger photon fluxes (compared to ion fluxes) can be generated. (See Fig. 1.) The time averaged ratio of photon-to-ion fluxes in ICPs can be controlled by varying the duty cycle of the pulsed plasma, aspect ratio of the reactor and gas pressure.

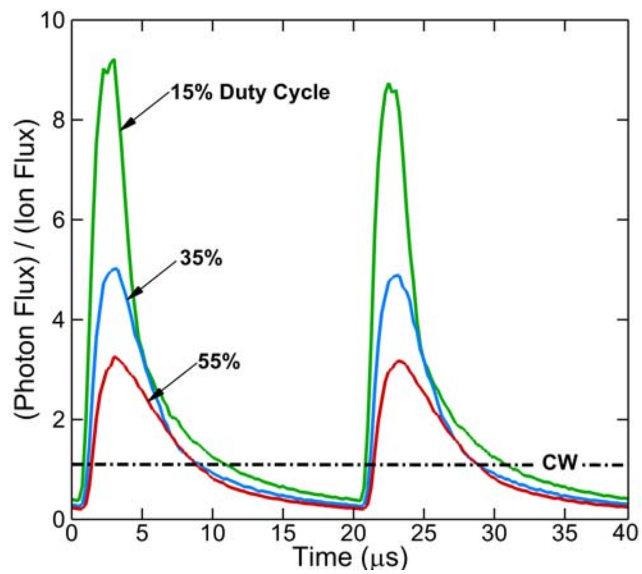

Fig. 1: Photon/Ion flux ratio of different duty cycles and CW power for an .Ar/Cl_2 plasma.

Work supported by Department of Energy Office of Fusion Energy Science, and the Semiconductor Research Corp.

3-10

Increasing Efficiency of Monte Carlo Particle-Fluid Collision Calculations on GPU

Charles Bardel, John Verboncoeur

Electrical and Computer Engineering, Michigan State University (bardelch@msu.edu, johnv@msu.edu)

Monte Carlo collision calculations for Particle-in-Cell codes can be a very computationally intensive procedure. Fortunately, this process can be set-up as an embarrassingly parallel problem for collisions with a background fluid, where the calculation of one particle does not rely on the results of another. This type of problem is well suited for GPUs, which could accelerate the computations an order of magnitude. One approach is to apply a function to every particle which involves computing the particle energy, a square root to obtain the speed, and either interpolation of tabled cross sections or computation of a curve fit for each process for every particle [1].

However, due to the nature of the hardware implementation of GPU, this simple straightforward implementation will not have the best performance fundamentally due to there being two different sets of particles: colliding and non-colliding. In this problem each of the launched groups of GPU threads, called warps, could contain members of each set of particles. Since the group is running together, the longest calculation in the group determines the running time of the entire group.

In order to achieve the best performance on the GPU the work of the particle groups to be computed must be load balanced so that the separate sub-tasks have approximately the same running time or operation count. This means that all the particles that will collide during time step must be known a priori. This can be achieved using the *null collisional method* [1] in which particles are selected at random using the total collision probability that is independent of particle energy and position.

On the GPU, memory requests, especially to 'Global memory,' are a very expensive operation. Based on memory access optimizations from the CUDA Best Practices Guide [2] its clear it would be best if the requested memory were collocated in memory within 128 Byte segments.

Since this memory optimization might severely impact the entropy of the collisions depending on the exact definition of what is meant for a particle to be collocated in memory. In this paper the memory mapping of the particles defined in [3] is used, which is designed for efficient particle-to-grid calculations.

In this paper two case studies are examined that utilize the optimizations, outlined above, for a fluid background gas model to examine statistical differences of selecting different sizes of collocated particles. The first simulation is uniformly distributed neutral particles initially at 0K with a fluid background collision model sampled from the Maxwell distribution. The second simulation adds a gravity well to ensure non-uniform density distribution of the particles.

References

[1] J. P. Verboncoeur, Plasma Physics and Controlled Fusion 47, A231 (2005).
[2] Nvidia, CUDA C Best Practices Guide, 2012.
[3] N. G. George Stantchev, William Dorland, Parallel Distrib. Comput. 68, 1339 (2008).

3-11

Parallelized Two-dimensional Particle-in-cell Simulation for Capacitively coupled Plasma Using Graphic Processing Unit

In Cheol Song , Seok Won Hwang and Hae June Lee

Pusan National University, South Korea (fepsong@pusan.ac.kr)

A large size chamber with 450 mm and plasma wall-interaction for the nano-scale feature are needed in semiconductor manufacturing industry recently. However, there are difficulties to experiment and simulate a large scale reactor chamber and nano-scale features. In the simulation case, plasma simulation using particle-in-cell (PIC) method shows very high accuracy compared with fluid simulations. However, PIC method has a disadvantage of slow speed caused by individual calculation of lots of computational particles. Recently, new computing method using graphic processing units (GPUs) enables to make a low-cost and low-power personal super computer and there is a study to utilize the GPUs for the parallelization of PIC plasma simulators [1,2]. To overcome the heavy computation problem of a PIC method, we have developed a parallelized PIC code using GPUs. In this work, two-dimensional axisymmetric simulator for a capacitively coupled plasma (CCP) sources is presented with the performance improvement using GPUs. Also, investigated were plasma phenomena with frequency variation as well as dual frequency with phase variation for CCP.

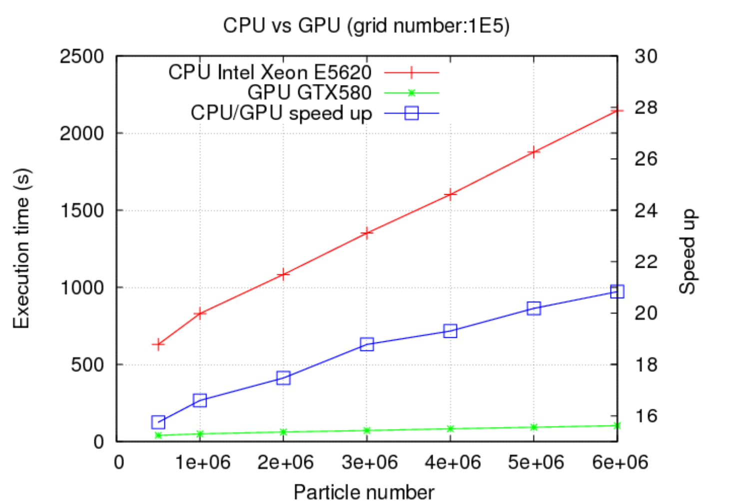

Fig.1: GPU-PIC code shows good performance. Single-GPU code is 20 times faster than single–CPU code.

References

[1] George Stantchev et al, J. Parallel Distrib. Comput. **68** ,1339–1349 (2008)

[2] R.G. Joseph et al, Parallel & Distributed Processing Symposium(IPDPS), pp.395-406 (2011)

3-12

Modeling of the O-X-B Double Conversion Process in Fusion Plasmas

M. Ali Asgarian [a, b], J. Verboncoeur [b] and A. Parvazian [a]

(a) Department of Physics, Isfahan University of Technology, Isfahan, Iran
(maliasgarian@ph.iut.ac.ir, parvazin@cc.iut.ac.ir)
(b) Department of Electrical and Computer Engineering, Michigan State University, USA
(maa@msu.edu, johnv@msu.edu)

Electron Bernstein waves (EBWs) are special electrostatic cyclotron waves which propagate with a short wavelength in hot plasma [1]. EBWs are useful for core plasma heating, current drive and temperature diagnostics in high density plasma devices like stellarators and tokamaks. The resonance of EBWs is close to the cyclotron harmonics, and they do not have a density cut-off. The ordinary-extraordinary-Bernstein (O-X-B) conversion is one of the processes for generating EBWs. The generated EBW propagates in the region with density higher than ordinary wave cut-off, $\omega = \omega_p$, and is strongly absorbed at the electron cyclotron harmonics, $\omega = n\omega_c$, for integer n . As such, EBWs may provide local electron heating and current drive.

This double conversion process has been simulated using the XOOPIC code. XOOPIC is a 2D PIC code with 3D electrostatic and electromagnetic field solvers for slab and cylindrical geometries [2]. The O-X-B simulation has been done in a slab plasma, using the electromagnetic field solver and a surface impedance wave source to generate the O-wave. The maximum energy efficiency in O-X conversion will be ensured with the optimized refractive index, parallel to the toroidal magnetic field $N_{\parallel,opt}$ [3]. Moreover, the dependence of the conversion efficiency on the density gradient scale length L_n will be considered [4]. The results compare well with published experiments [5] and the results of full-wave simulation codes [6].

References

[1] I. B. Bernstein, Physical Review **109**, 10 (1985)
[2] J. P. Verboncoeur, et al., Computer Physics Communications **87**, 199 (1995)
[3] J. Preinhaelter and V. Kopecky, J. Plasma Physics **10**, 1 (1973)
[4] F. R. Hansen, et al., J. Plasma Physics **39**, 319 (1988)
[5] V. Shevchenko, et al., Fusion Science and Technology **52**, 202 (2007)
[6] A. Kohn, et al., Plasma Phys. Control. Fusion **50**, 085018 (2008)

3-13

Spreading Resistance of Thin Film Contacts

Peng Zhang, Y. Y. Lau, and R. M. Gilgenbach

Department of Nuclear Engineering and Radiological Sciences
University of Michigan, Ann Arbor, MI 48109-2104

Electrical contact [1] is important to integrated circuits, thin film devices, carbon nanotube based cathodes, interconnects, field emitters, wire-array z-pinches, metal-insulator-vacuum junctions, and high power microwave sources, etc. Contact resistance is also critical to micro-electromechanical system (MEMS) relays and microconnector systems, where thin metal films of a few microns are typically used to form electrical contacts. The crowding of the current lines at contacts leads to enhanced localized heating, a measure of which is the spreading resistance (R_s). For a microscopic area of contact (the "*a*-spot" [1]) on a thin film, we calculate R_s in both Cartesian and cylindrical geometries [2]. In the limit of small film thickness, *h*, the normalized thin film spreading resistance converges to the finite values, 2.77 for the Cartesian case and 0.28 for the cylindrical case. These same finite limits are found to be applicable to the *a*-spot between bulk solids in the high frequency limit if the skin depth is identified with *h*. Extension to a general *a*-spot geometry is proposed [2].

Figure 1a shows the Cartesian (cylindrical) geometry of electrical contact between two thin films of the same material. Figure 1b shows the normalized spreading resistance in one of the contact thin films for the cylindrical geometry of Fig. 1a. It is clear that the normalized thin film spreading resistance converges to 0.28 as $h \rightarrow 0$. The calculation is confirmed with MAXWELL 2D simulation.

Work supported by an AFOSR grant FA9550-09-1-0662, L-3, Northrop-Grumman.

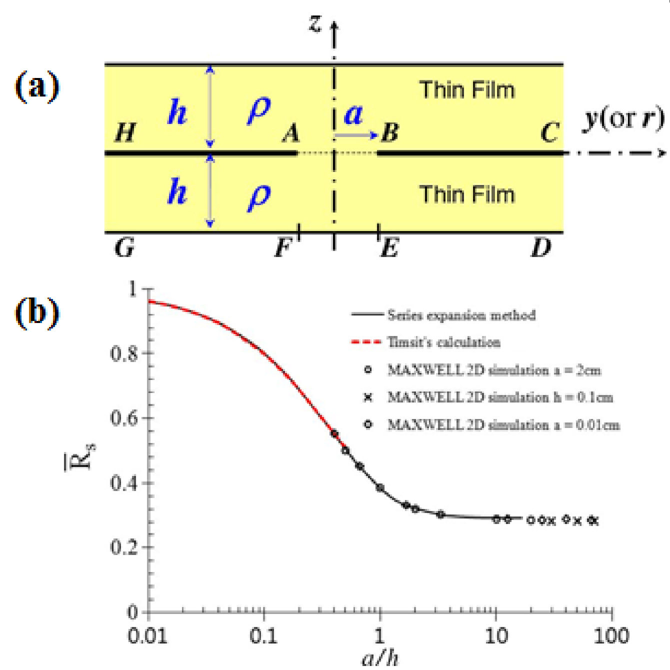

Fig. 1: (a) Thin film contact structures in either Cartesian or cylindrical geometries. (b) The normalized contact resistance for cylindrical thin film structures in (a), as a function of aspect ratio *a*/*h*. the solid line is for the series expansion calculation, the dashed line is for Timsit's calculation; and the symbols are for MAXWELL 2D simulation [2].

References
[1] R. Holm, Electric Contacts, 4th ed., Springer (1967).
[2] P. Zhang et al., IEEE Trans. Electron Devices **59**, 1936 (2012).